

# A model for global cooperation on climate change: Dynamic Lindahl equilibrium under uncertainty

Markku Kallio, Iivo Vehviläinen, and Hanna Virta\*

May 2, 2023

## Abstract

We study the value of a cooperative solution to the global climate externality problem in a world that is uncertain and dynamic. Our analysis incorporates negative emissions technologies that seem critical to resolve the crisis, especially if the climate future proves catastrophic. We generalize earlier theoretical results for Lindahl’s equilibrium, and integrate with an up-to-date version of Nordhaus’s pioneering RICE-model to quantify regional economic impacts. Low-income regions end up with the highest relative value of cooperation through three distinct channels: lower damages, equilibrium compensations, and burden sharing of abatement actions.

**JEL Classification:** C61, D61, D81, Q54, Q58

**Keywords:** climate–economy model, Lindahl’s equilibrium, international cooperation, negative emission technologies

---

\*Kallio (markku.kallio@aalto.fi): department of information and service management Aalto University, Vehviläinen (corresponding author: iivo.vehvilainen@aalto.fi): economics department Aalto University and Helsinki Graduate School of Economics, Virta (hanna.virta@vtv.fi): National Audit Office of Finland. An earlier version of the paper, “Dynamic Lindahl equilibrium under uncertainty: A model for global cooperation on climate change”, was published as part of Hanna Virta’s PhD Thesis in 2014. We are grateful to William Nordhaus and Zili Yang for RICE2020 model and data. We thank Daniel Hauser, Niko Jaakkola, Eero Kasanen, Markku Kuula, Matti Liski, Peter Matthews, Pauli Murto, Esa Tommila, and Juuso Välimäki, and participants at seminars in Helsinki, IIASA, and Turku for valuable comments and discussions.

# 1 Introduction

“Here, in Paris, we can show the world what is possible when we come together, united in common effort and by a common purpose.”

—Barack Obama, speaking to the COP21.

International negotiations on climate change are challenged by conflicting interests among stakeholders and trade-offs between future uncertainty and the short-term costs of action. This article addresses both these concerns jointly. In particular, we study the value of cooperation and explore the returns of far-reaching technologies that could cushion the most disastrous climatic outcomes. We evoke Lindahl’s solution as our cooperative equilibrium concept in a setting where multiple regions dynamically adjust to an uncertain climatic future, and quantify outcomes.

Reaching an agreement on global climate change policy is particularly convoluted because of uncertainty that stems from three distinct channels: 1) nature reveals the impacts of today’s emissions on climate with a delay, 2) economic damages in the out-of-sample future are hard to predict, and 3) the possibilities of novel future technologies to resolve the crisis remain under-explored. Both climate change impacts and the initial economic endowments are heterogeneous across regions, adding to tensions in the labyrinthine negotiations. Our model is motivated by the possibility to include uncertainties explicitly: trying to reach consensus on, e.g., a global carbon tax, is bound to be more difficult than agreeing on the potential range of outcomes and available responses<sup>1</sup>. We thus agree with Barnett, Brock and Hansen (2022) that “. . . uncertainty considerations should remain as first-order concerns and not be shunted to the background as they often are in policy discussions”.

Lindahl’s solution to the public good allocation problem is to find a global level of taxes that everyone agrees on, given the personalized reimbursements that the collected taxes fund. Our theoretical contribution is to generalize the static and deterministic early results on Lindahl equilibrium – the seminal papers in the context of climate change are Chichilnisky, Heal and Starrett (1993); Chichilnisky and Heal (1994); Mäler and Uzawa (1994) – to a world that

---

<sup>1</sup>E.g., Battaglini and Harstad (2020) show how political economy considerations limit the ability to commit to strong climate treaties.

is dynamic and uncertain and consensus is sought over time and over a variety of potential states of nature<sup>2</sup>. We implement carbon pricing through a tradeable emissions permit system that enables smoothing of consumption across regions and we include financial markets for smoothing over time. Unanimity on permit prices in each contingency over time determines the global emissions reduction ambition. Our solution concept is based on Negishi (1972)’s existence proof of the competitive equilibrium: We formulate the equilibrium conditions of Lindahl’s allocation as a social welfare maximization problem, with appropriately weighted regional utilities, and prove the existence of the equilibrium<sup>3</sup>. We show that the resulting equilibrium can implement the first-best solution, at least under reasonable assumptions about the economic and climate primitives<sup>4</sup>. Notably, Lindahl’s equilibrium also gives us well-founded motivation for social planner’s weighting of regional utilities.

The theoretical conceptualizations above lead to a computationally non-trivial exercise. Stakeholders’ equilibrium willingness-to-pay values depend on intricate climate–economy interactions that need to be solved simultaneously with the equilibrium conditions. Our empirical approach is novel and offers gains in versatility and transparency over the past literature. We opt for the RICE model (Nordhaus and Yang, 1996, 2021) as our point of departure as it provides an established calibration of the climate and economic interdependencies, sufficient for our quantitative aims<sup>5</sup>. Our closest correspondence in building a dynamic integrated-assessment model with uncertainty and heterogeneous regions is with Hassler and Krusell (2012), yet they rely on a more stylized model and abstract away from global equilibrium solutions. More recent work has abstracted away from uncertainties to

---

<sup>2</sup>We abstract away from incentives of the parties to do so, see, e.g., Hoel and Schneider (1997) and Weikard, Finus and Altamirano-Cabrera (2006).

<sup>3</sup>We construct the proof directly. The existence of static Lindahl’s equilibrium in Foley (1970) follows from general equilibrium concepts: Public goods are included in consumption bundle, and then the “public competitive equilibrium” can be defined for general economies, including non-convex ones (see Murty, 2010).

<sup>4</sup>Conceptually this is not surprising: Lindahl’s equilibrium is connected to efficiency in static and deterministic climate applications (Chichilnisky, Heal and Starrett, 1993), in design of efficient compensation mechanisms (Varian, 1994), and in efficient uniform price auctions for public goods where an optimal VCG mechanism can be given an interpretation of Lindahlian flavor (Montero, 2008).

<sup>5</sup>Despite the simple structure of RICE, as shown by, e.g., Golosov et al. (2014); Gerlagh and Liski (2016), even more compressed models can be sufficient to capture key climate dynamics.

either focus on key economics, as in, e.g., Barrage (2020) who studies the question of optimal carbon taxes in the presence of other distortionary taxes, or more detailed climate models, see, e.g., Krusell and Smith (2022); Cruz and Rossi-Hansberg (2023). Our aim is for the middle ground, keeping the foundations of the well-known RICE model mostly intact even as we incorporate the latest research on key climate and economic uncertainties.<sup>6</sup>

Our main contribution is to the study of negative emissions technologies that could shape the environmental state directly. Though these technologies seem like science fiction today, they appear to be instrumental especially in catastrophic climate outcomes. We use a flexible probabilistic representation, a model that has path dependent draws for the state of nature realized over time, to capture the possibility of a catastrophe over the current range of plausible estimates of key uncertainties<sup>7</sup>. One can interpret the catastrophe as a sudden substantial markdown in the carbon budget available for a relatively safe climate future; the increased scarcity then necessitates a more immediate response from a backstop technology (see Nordhaus, 1973; also Liski and Murto, 2006).

Our integrated assessment model reproduces many of the earlier findings. First, while global emissions fall, the slow removal of current carbon stocks leads to a warming planet (e.g., Rogelj et al., 2019), and even ambitious reductions in emissions/output ratios appear insufficient to meet climate targets – still true in a cooperative solution. Second, as in, e.g., Lemoine (2021), we find that uncertainty increases the social cost of carbon; however, this result is diluted if negative emissions technology is successfully deployed as the adverse tail of the outcomes is removed. Third, like, e.g., Crost and Traeger (2014), we find uncertainty about economic damages less relevant than uncertainty about temperature sensitivity. These results hold true in Lindahl’s equilibrium, in which the economic and environmental impacts seem identical with the first-best allocation in our configurations<sup>8</sup>; however, the social planner is indifferent to the distribution of consumption among the world regions.

The literature on quantitative comparisons between cooperative and non-cooperative

---

<sup>6</sup>We use an updated model for climate dynamics, as in Barnett, Brock and Hansen (2022), we use Geoffroy et al. (2013) as the starting point; see also Dietz et al. (2021). Also, we favor more stringent economic damages than the default polynomial form in RICE, and opt for exponential damages akin to Weitzman (2009).

<sup>7</sup>This formulation follows naturally from stochastic programming, see, e.g., Wets (1989).

<sup>8</sup>See Shiell (2003) for a discussion.

allocations has been thin.<sup>9</sup> Perhaps surprisingly, the present value of the expected aggregate over-time consumption in Lindahl’s allocation is only marginally higher than in Cournot–Nash competition between the regions in moderate climatic futures. However, compared to the cooperative equilibrium, competing regions consume more and abate less in the short-term, exposing them to damages that are greater later on, especially if an adverse draw from climatic uncertainties is realized. In our baseline configuration, damages in a catastrophic scenario wipe out around half of global output by the mid 22nd century if regions continue to compete against each other, whereas the damages are “only” around one-third in the cooperative solution. The relative gains from cooperation differ between regions; however, all regions gain, particularly some of the poorest parts of Africa and Asia.

Our main novelty is to allow for a negative emissions technology and study its global and regional impacts under uncertainty<sup>10</sup>. Strikingly, in the non-cooperative solution, the high-income regions free-ride on the abatement actions of the poorer regions as the high-income regions mostly are also the ones most resilient to the warming climate<sup>11</sup>. As in the global analysis of Cai and Lontzek (2019), high damages in the catastrophic scenario imply high insurance value to the new technology. Depending on the probability of successful technology deployment, the present value of a negative emissions technology is in trillions of U.S. dollars in the cooperative solution. If no agreement is reached, the regions that face the highest damages will be forced to employ negative emissions technology, but this enforces the free-riding potential of the high-income regions. In the cooperative regime, high-income regions contribute to the uptake of the technology much earlier, leading to shared benefit from the improved state of the environment.

Combined, our results point to several policy implications: 1) cooperation improves efficiencies at least close to the first best level, 2) not cooperating contributes to worsening

---

<sup>9</sup>Kotchen (2018) and Groot and Swart (2018) share some of our research motivations but operate with more stylized models, as do Van der Ploeg and de Zeeuw (2016) who study the differences with a two region model.

<sup>10</sup>We study Direct Air Capture (DAC), one potential future technology, see, e.g., National Academies of Sciences (2019). Note that while DAC technologies share the benefits of geoengineering, they seem less risky, cf. Barrett (2008).

<sup>11</sup>Like in the more stylized model of Jaakkola and Van der Ploeg (2019).

climate conditions that wipe out the economic gains from the short-term use of additional emissions, 3) redistributions can make all regions better off with Lindahl’s allocation compared to the non-cooperative outcomes, and 4) benefits from cooperation are large for the more vulnerable regions. Finally, a general interpretation of the results is that the rich countries could fund the public good technology development as a politically acceptable contribution to a global climate agreement. As a related example, the U.S. recently allocated \$3.7 billion for such technology development<sup>12</sup>.

Finally, the list of caveats to our quantification is long and well-documented. First thing to note is the choice of discounting rate; our main analysis is done with 3%, a lower value would place a higher weight on future generations’ welfare. For a critical discussion of the other modeling assumptions in integrated assessment models, see Pindyck (2013), which we subscribe to, to a large extent. Switching to a more modern economic model could provide a deeper view on the mechanisms of adaptation to the changing climate in areas such as endogenous technology growth, energy sector involvement, migration, or trade, but a universally accepted way into incorporate all these aspects to one single model is still lacking<sup>13</sup>. We also steer clear of the discussion on the uncertainty about uncertainty as other emerging work is documenting the implications<sup>14</sup>. We reemphasize the scope of our quantification: it is not to learn about a precise tax level that shall never be globally implemented, but to understand the interplay between regional tensions, uncertainty, and the possibility of new negative emissions technologies.

The paper proceeds as follows. We start with a stylized illustration in Section 2. Section 3 introduces the theory and computation of dynamic Lindahl equilibrium under uncertainty. Section 4 discusses the computational results and Section 5 concludes. All proofs are in Appendix D, and Online Appendix B explains how the RICE-2020 model is adapted to implement our Lindahl equilibrium model.

---

<sup>12</sup>Funding to develop carbon dioxide removal industry (source: U.S. DOE, 22 Dec 2022).

<sup>13</sup>See, e.g., Gillingham et al. (2018).

<sup>14</sup>E.g., Jensen and Traeger (2021) in addition to Barnett, Brock and Hansen (2022).

## 2 Static illustration

### 2.1 Lindahl's equilibrium

Lindahl (1919)'s proposition was based on the ideal of a political bargaining protocol where all sensible actors would reach unanimity on the level of public good provision and its financing. We will use the following interpretation of Lindahl's equilibrium. While the theory is applicable in more generality, we are steered by our climate setting: Regions produce with a polluting technology to enjoy private consumption but face a common global externality that reduces output. Each region chooses its own level of production that results in a negative global externality that can be reduced with costly abatement actions. We also assume the existence of an international market for tradable pollution permits and financial markets.

*Lindahl's equilibrium.* Four conditions hold in all states of nature over time: (1) regions reach unanimity on preferred global emissions, (2) local production decisions are consistent with global emissions, (3) net emission charges sum up to zero, and (4) financial positions are globally balanced.

The behavioral assumptions behind Lindahl's solution are strong: the parties report their preferences truthfully and everyone commits to its implementation. As critiqued by Samuelson (1954), such information disclosure is not in everyone's best interest, breaking down the equilibrium. Also, with global problems, outside intervention cannot be provided, which makes it difficult to sustain agreement over the extended time span required (see, e.g., Baliga and Maskin, 2003). To counterbalance Samuelson's criticism, we argue that the quantified Lindahl's solution, with uncertainties, can help to structure climate negotiations as no party has superior private information on their valuations over the coming decades and centuries. Moreover, our results suggest that if the compensations required are paid as investments in technology development, shorter commitment periods may suffice.

### 2.2 Static and deterministic model of two regions

To fix ideas, consider first a highly stylized climate version of Lindahl's original idea. The planet is divided into two regions, the North and the South. The output of region  $i$  is given

by  $y_i = y_i(k_i, l_i, e_i, x)$  with capital  $k_i$ , labor  $l_i$ , and emissions  $e_i$  as inputs. Production is heterogeneously affected by the global state of the environment  $x$  that deteriorates based on total emissions  $e = \sum_i e_i$  with some rate  $f$ . For the regions, reducing emissions is increasing costly; hence,  $y_i$  is increasing with  $e_i$ . Consumption of region  $i$  is  $c_i$ , yielding per capita utility  $u(c_i/l_i)$  where the utility function is assumed to be concave. In the static model without transfers, all output is consumed immediately and we have  $c_i = y_i$ .

Lindahl's solution is to seek unanimity on the state of the global climate, in this stylized illustration determined directly based on the level of total emissions, and to agree on the burden sharing of the costly actions required to mitigate the externality. We construct Lindahl's equilibrium through two variants of cooperation: First, we start with a world where cooperation is possible but emissions trading is not, i.e., conditions (1) and (2) above are fulfilled. Second, we show how a combination of emissions pricing and compensations can be used to reach efficiency, even as we require that condition (3) is also met. The full model in use from Section 3 onward is with emissions pricing and compensations, and includes financial markets for the over-time smoothing of consumption.

To see how Lindahl's equilibrium is reached in the simple setup, let both regions report their desired level of total emissions,  $e$ , as a function of the share of the total emissions they can use for their private production; in effect regions agree on a global emissions quota and its regional allocation. Figure 1 offers an illustration where a growing share of emissions is allocated to the North and the remainder to the South<sup>15</sup>. Given a fixed quota, each region will choose a level of output that trades-off its marginal cost of abatement  $\partial y_i / \partial e_i$  with marginal damages from the deteriorating state of the environment  $\partial y_i / \partial x$ . Initially, the larger the quota a region receives, the larger the total emissions it is willing to accept, but the trend can reverse if marginal costs differ; in Figure 1 the preferred emissions of the North decline with higher allocations as abatement is costlier for it than the South. However, if the non-convexities related to the externality are weak enough in the relevant subset of possible production decisions, there is a unique equilibrium allocation of emissions so that the choice of global emissions is unanimous, this is Point A in Figure 1.

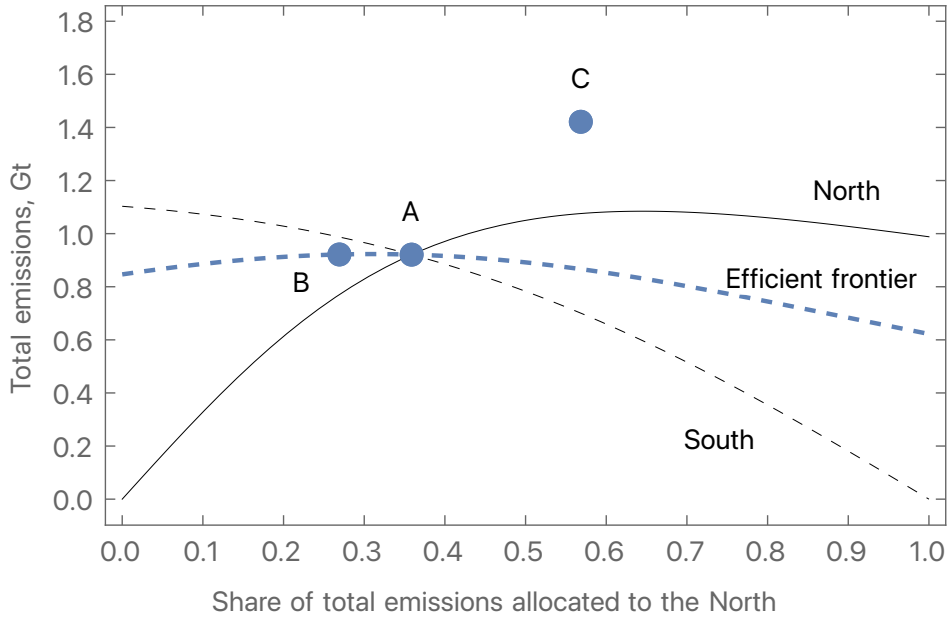
The first-best solution may deviate from cooperative equilibrium as the planner maxi-

---

<sup>15</sup>Online Appendix A provides details of the primitives and computations used in Figure 1



**Figure 1:** Lindahl's equilibrium



Notes: Solid line represent the desired emissions of the North and the thin dashed line of the South as a function of the allocation between the two regions (0 = all emissions are allocated to the South, 1 = all emissions are allocated to the North). Efficient frontier (bold blue dashed line) shows the emission quota that a social planner would choose given the allocation of the quota between the regions. Point A is the agreed allocation if transfers are not possible. Point B is Lindahl's equilibrium that includes emissions trade and implements also the first-best. Point C is the non-cooperative Cournot-Nash equilibrium.

mizes output by allocating abatement actions so that marginal costs equalize across regions. Here social planner's allocation, Point B in Figure 1, increases the aggregate consumption, and utility, over the first cooperative equilibrium (Point A). As is well-known, if lump-sum transfers are not available across national borders, the traditional separation between equity and efficiency breaks down on policies for global public goods (see, e.g., Sandmo, 2003)<sup>16</sup>, but allowing for indirect transfers via emissions pricing may or may not be sufficient to support the efficient allocation<sup>17</sup>. Cost sharing can proceed as follows: regional emissions  $e_i$  are taxed

<sup>16</sup>Though the discussion here is disguised under neutral terms, the choice of an equilibrium concept is a normative one: In Lindahl's solution the initial endowments of stakeholders are taken as given, see e.g. Stanton (2011) for a discussion. Other equity considerations could be included as well (see, e.g., Anthoff and Emmerling, 2019 for global equity questions), but we entertain no such causes for this paper.

<sup>17</sup>The static case is analyzed in Chichilnisky, Heal and Starrett (1993). Also Varian (1994) discusses the sufficiency of linear pricing to sustain the first-best equilibrium.

at a global rate  $P$  and each of the regions gets compensation,  $P_i e$ , based on total emissions  $e$  at personalized rates  $P_i$ . In equilibrium, tax finances compensations so that  $\sum_i P_i = P$  because  $\sum_i e_i = e$ . This is Lindahl's equilibrium: regions agree on 1) the level of global emissions  $e$ , 2) their regional production decisions are aligned with the total emissions, and 3) the emissions charges sum up to zero. There is no difference between Lindahl's solution and the planner's allocation in this static case, and the differences are minute even in our full model; we elaborate on this below.

The non-cooperative solution, where regions compete à la Cournot, leads to substantially higher emissions than the cooperative allocation. Each region makes an independent output decision based on the same trade-off between the marginal cost of abatement and global damages but with no regard to the allocation of emissions between the regions. If best response functions are concave, again at least empirically in the relevant part of the strategy space, a unique pure strategy Nash equilibrium is found; see Point C in Fig. 1. In this stylized illustration, the gains from self-serving production decisions lead to lower total output than in the cooperative solution, but the distributional impacts are heterogeneous; in the numerical example the North gaining at the expense of the South.

Final step is to show how the equilibrium tax and compensation prices in Lindahl's allocation are determined. In the stylized model used in Fig. 1, the prices can be derived analytically, but this does not hold for more complex settings. Following Negishi (1972), we show how the equilibrium conditions of Lindahl's allocation coincide with the following social welfare maximization problem with appropriately selected weights  $\lambda_i$  for the utilities of the regions:

$$\begin{aligned} & \max \sum_i \lambda_i u_i(c_i/l_i) \\ & s.t. \\ & \sum_i (c_i - y_i) = 0 \quad (d) \\ & -x + f \sum_i e_i = 0 \quad (\mu) \end{aligned}$$

where  $d$  is the shadow price associated with the budget balance constraint and  $\mu$  with the environmental state equation. Denoting with  $u'_i = \partial u_i / \partial c_i$ ,  $y_i^e = \partial y_i / \partial e_i$ , and  $y_i^x = \partial y_i / \partial x$ ,

optimality (dual feasibility) requires

$$\lambda_i u'_i = d, \quad dy_i^e = \mu f \quad \text{and} \quad d \sum_i y_i^x = -\mu.$$

Given a global emissions tax  $P$  and a compensation price  $P_i$ , the problem of region  $i$  is to find consumption  $c_i$ , output  $y_i$ , local emissions  $e_i$ , global emissions  $e$  preferred by  $i$ , and environmental state  $x$  to

$$\begin{aligned} & \max \lambda_i u_i(c_i/l_i) \\ & s.t. \\ & c_i - y_i + P e_i - P_i e = 0 \quad (d_i) \\ & -x + f e = 0 \quad (\mu_i) \end{aligned}$$

where  $d_i$  and  $\mu_i$  are shadow prices, and optimality requires

$$\lambda_i u'_i = d_i, \quad P = y_i^e, \quad d_i y_i^x = -\mu_i \quad \text{and} \quad d_i P_i = \mu_i f.$$

In equilibrium, the Negishi weights  $\lambda_i$  are such that optimal  $c_i$ ,  $y_i$ ,  $x$ ,  $e_i$  and  $e = \sum_i e_i$  for the global problem are optimal for the local problems as well. Then the following conditions must hold: i) the marginal value of consumption across regions is equal,  $d_i = d$ , ii) the marginal value of emissions reductions globally normalized with the marginal value of consumption gives the global tax,  $P = \mu f/d$ , iii) the normalized marginal value of emissions reductions for the region gives the compensation rate  $P_i = \mu_i f/d$ , and iv) budgets balance in all regions  $c_i - y_i + P e_i - P_i e = 0$ . The first three conditions follow from optimality conditions of the global and local problems. In Section 3.3 we propose an algorithm to find weights  $\lambda_i$  for resolving the budget issue. Such optimal solutions for the local problems constitute a Lindahl equilibrium satisfying the conditions stated above. The next Section shows that the principles above carry to the dynamic and stochastic models as well.

### 3 Dynamic Lindahl equilibrium under uncertainty

Generalization of Lindahl's equilibrium to a setting where multiple regions make state dependent production decisions over time requires several steps<sup>18</sup>. We continue by first introducing how uncertainty is brought into the model in Section 3.1. In Section 3.2, we describe the optimization problem each of the regions faces and state the equilibrium conditions. Section 3.3 introduces the global problem and includes the main theory for the existence and efficiency of Lindahl's equilibrium as well as the computational algorithm to find one. Finally, Section 3.4 shows how emissions trading is incorporated into the model.

#### 3.1 Preliminaries for dynamic and stochastic models

We employ a discrete time approach, where  $T$  periods are defined by time stages  $t = 0, 1, \dots, T$ ; i.e., the time horizon is subdivided into  $T$  periods. An index  $t < T$  also refers to a period between stages  $t$  and  $t + 1$ . For convenience, let the time span of period  $t$  be a constant  $\Delta$ .

Uncertainty is captured by a discrete set of states of nature at each time stage. The realizations of uncertainties are path dependent so that over time they are represented by a scenario tree; for an example, see Figure 2. We adopt the following simplifying notation. Let  $n \geq 0$  denote a node of the scenario tree with  $n = 0$  referring to the root. For  $n \neq 0$ , let  $n_-$  denote the predecessor of node  $n$ . Let  $E$  be the set of terminal state nodes in stage  $T$  and  $F$  the set of final control nodes in stage  $T - 1$ . For all nodes  $n$ , let  $n_+$  denote an immediate successor node of  $n$  and let  $S_n$  be the set of all such successor nodes  $n_+$ . For terminal nodes  $n \in E$ ,  $S_n$  is an empty set. Hence, for all  $s \in S_n$ , we have  $s_- = n$ . If node  $n$  appears at stage  $t$  then the predecessor node  $n_-$  is at stage  $t - 1$ , and the successor nodes  $n_+ \in S_n$  are at stage  $t + 1$ . A node  $n$  in stage  $t < T$  also refers to a period between stages  $t$  and  $t + 1$  starting with  $n$ ; for example, emissions in node  $n$  refers to emissions during the period. The probability of attaining node  $n$  is  $\pi_n > 0$ , for all  $n$ .

---

<sup>18</sup>Earlier generalizations of Lindahl's solution exist, for instance, in Foley (1970), Kaneko (1977), and Mas-Colell and Silvestre (1989), but they do not cover our setting.

### 3.2 Equilibrium conditions

Before writing Lindahl's equilibrium conditions for the global allocation problem we describe how the local interests of stakeholders are formed. Consider the world subdivided into  $N$  regions  $i = 1, 2, \dots, N$ . Preferences of region  $i$  are characterized by the expected utility of a stochastic consumption stream over time. If vector  $c_i = (c_{it})$  denotes a deterministic consumption stream, such that  $c_{it} \geq 0$  is the level of consumption of region  $i$  in period  $t$ , for  $t = 0, 1, 2, \dots, T - 1$ , then an additive utility function of region  $i$  is

$$u_i(c_i) = \sum_{t < T} \rho_{it} v_i(c_{it}), \quad (1)$$

where  $\rho_{it}$  is an exogenous parameter accounting for time preference and  $v_i(c)$  is a utility function. We assume the following:

**Assumption A0:** Utility functions  $v_i(c_i) \in C^1$  are increasing and strictly concave, with  $v'_i(c_i) \rightarrow \infty$  as  $c_i \rightarrow 0$ .

The state of global environment at node  $n$  is given by vector  $x_n$ . In the climate application, component  $x_{a,n}$  denotes the average atmospheric temperature above the pre-industrial level and  $x_{c,n}$  the global atmospheric  $CO_2$  concentration. Other components of  $x_n$  may include average ocean temperature and carbon stocks in land and oceans. The level of  $CO_2$  emissions  $e_{in}$  of region  $i$  in node  $n \notin E$  is endogenous. Given global emissions  $e_n = \sum_i e_{in}$ , the state  $x_n$  of the global environment is incremented by  $f e_n$ , where the column vector  $f$  is a unit vector with a component 1 assigned to increment the atmospheric carbon  $x_{c,n}$ . For the local problem,  $e_n = e_n^i$  denotes the global emissions preferred by region  $i$ . The impact of the preceding state  $x_{n-}$  during the period is given by a continuously differentiable vector valued function  $M(x_{n-})$  so that the state dynamics is given, for all nodes  $n$ , by

$$-x_n + M(x_{n-}) + f e_{n-}^i = g_{n-} \quad \forall n \quad (\mu_{in}). \quad (2)$$

where  $g_{n-}$  is exogenous. The initial state  $x_0$  is exogenously fixed; it is formally defined in (2) by exogenous preceding levels  $x_{0-}$ ,  $e_{0-}$  and  $g_{0-}$ . Parameter  $\mu_{in}$  is the vector of dual variables of constraint (2) of the local optimization problem.

Let  $y_{in}$  denote the output per period of the consumption good in region  $i$  at node  $n \notin E$ . The output satisfies

$$y_{in} - \psi_{in}(k_{in}, l_{in}, e_{in}, x_{a,n}) \leq 0 \quad \forall n \notin E \quad (\eta_{in}). \quad (3)$$

where the production function  $\psi_{in}$  depends on an exogenous labour  $l_{in}$  and three endogenous attributes: capital stock  $k_{in}$  and the emissions  $e_{in}$  of region  $i$ , and average global atmospheric temperature  $x_{a,n}$  whose increase causes damage losses. Above,  $\eta_{in}$  is the dual variable of the equation (3) in the local optimization problem.

**Assumption A1:** Production functions  $\psi_{in}(k_{in}, l_{in}, e_{in}, x_{a,n})$  are strictly concave, strictly increasing in  $k_{in}$ ,  $l_{in}$  and  $e_{in}$ , strictly decreasing in  $x_{a,n}$ , and differentiable with continuous partial derivatives.

In each node  $n \notin E$ , investments  $z_{in}$  increment the capital stock at node  $n_+ \in S_n$ . Due to depreciation, capital stock at the predecessor node depreciates during the period by factor  $\delta_k$ ,  $0 < \delta_k < 1$ . Hence, the capital stock dynamics of region  $i$  is given, for all nodes  $n$ , by

$$k_{in} - \delta_k k_{in_-} - z_{i,n_-} = 0 \quad \forall n \quad (\nu_{in}) \quad (4)$$

where the initial capital stock  $k_{i0}$  in (4) is exogenous defined by  $k_{i0_-}$  and  $z_{i,0_-} = 0$ , and  $\nu_{in}$  denotes the dual variable of the constraint (4) in the local optimization problem.

For all  $n \notin E$ , let  $P_n$  denote the price used to charge region  $i$  for its emissions  $e_{in}$  and  $P_{in}$  the price to compensate region  $i$  for global emissions  $e_n$ . Hence, the net payments of charges and compensations, the side-payments, contributed by region  $i$  at node  $n$  are  $P_n e_{in} - P_{in} e_n$ . Lindahl prices  $P_{in}$  and  $P_n$  are determined by Lindahl's equilibrium, and in the local problem they are taken as given.

Financial markets may include a single period risk free asset (bank account), which can be used for lending (saving) or borrowing. Additionally, depending on the stage and state (node), there may be several risky assets. We assume that the market is perfect. In this case there are no market frictions, such as transaction costs, nonzero interest rate margin between borrowing and lending, costs or restrictions on short positions. Additionally, assume that the financial market is complete. To summarize:

**Assumption A2: Financial market** is perfect and complete.

There are  $|S_n|$  successor nodes of node  $n$ . Hence, it follows from Assumption A2 that there are at least  $|S_n|$  assets for financial investment at node  $n$ . These may consist of a risk free asset and risky assets, such as futures or forward contracts on emission permits, for instance. For financial investments, let  $s_{in}$  be the column vector of endogenous investment positions (levels of investments) taken by region  $i$  at node  $n \notin E$ . Let the row vector  $B_n$  denote the unit values (prices) of assets at node  $n$  and let the row vector  $Q_{n_+}$  denote the unit values at successor node  $n_+ \in S_n$ . Hence, given investment  $s_{in}$ , the investment cash flow at node  $n$  is  $-B_n s_{in}$  and at node  $n_+ \in S_n$  the resulting cash flow is  $Q_{n_+} s_{in}$ . Given investment  $s_{in_-}$  at the predecessor node of node  $n$ , the total investment cash flow at node  $n$  is  $-B_n s_{in} + Q_n s_{in_-}$ . The initial vectors  $B_0$  and  $Q_0$  are exogenous.

Vectors  $B_n$  and  $Q_n$  are determined by a competitive market equilibrium, and they are exogenous for regional optimization problems. For example, if a single period risk free asset exists at node  $n$  with total return  $R_n$ , we may define its component in  $B_n$  to be equal to one so that the cash flow component in  $Q_{n_+}$  is  $R_n$ , for all  $n_+ \in S_n$ . Total return  $R_n$  is endogenously determined by an equilibrium.

As another example, suppose a single period forward contract on emissions permits with a forward price  $F_n$  is one of the risky assets at node  $n$ . Then its component in  $B_n$  is equal to zero and the cash flow component in  $Q_{n_+}$  is the difference of the emissions price at  $n_+ \in S_n$  and the forward price  $F_n$ , both of which are endogenously determined in an equilibrium.

Taking into account production, consumption, capital stock investments, financial investments, and side-payments (emission charges and compensation based on desired global emissions  $e_n = e_n^i$ ), the budget balance constraint for region  $i$ , for all nodes  $n \notin E$ , is

$$c_{in} + z_{in} - y_{in} + P_n e_{in} - P_{in} e_n^i + B_n s_{in} - Q_n s_{in_-} = 0 \quad \forall n \notin E \quad (d_{in}). \quad (5)$$

Parameter  $d_{in}$  is the dual variable of the budget constraint. For the root node  $n = 0$ , the prices  $B_0$  and  $Q_0$  are given, and the preceding financial investment position  $s_{i0_-}$  is exogenous. For instance,  $s_{i0_-}$  may be an initial debt which can be renewed at  $n = 0$ . However, we require the debt to be in balance over the entire horizon of  $T$  periods. Therefore, for end nodes  $F$  we require

$$s_{in} = 0 \quad \forall n \in F. \quad (6)$$

For subsequent use, we scale the expected utility of each region  $i$  by weights  $\lambda_i > 0$  with  $\sum_i \lambda_i = 1$ . The weights  $\lambda_i$  will be used in the Negishi iteration when we seek the global equilibrium. Summarizing (1) - (6), the *local problem*  $i$  is as follows: Given Lindahl prices  $P_{in}$  and  $P_n$ , and financial market data  $B_n$  and  $Q_n$ , find  $c_{in}$ ,  $y_{in}$ ,  $z_{in}$ ,  $k_{in}$ ,  $e_{in}$ ,  $e_n^i$ ,  $x_n$  and  $s_{in}$  to

$$\begin{aligned} \max \lambda_i \sum_{n \notin E} \pi_n \rho_{in} v_i(c_{in}) \\ \text{s.t. (2) - (6).} \end{aligned} \quad (7)$$

**Lemma 1.** *Assume A0 holds and an optimal solution exists for each regional problem (7). Then the weights  $\lambda_i > 0$  can be chosen such that the optimal dual variables  $d_{i0} = d_0$  at the root node are equal for all regions, and subsequently, Assumption A2 implies that the optimal dual variables  $d_{in} = d_n > 0$ , for all nodes  $n \notin E$ , are independent of regions.*

**Definition 1. Lindahl equilibrium conditions.** *An equilibrium prevails if the prices  $P_{in}$  and  $P_n$  and financial market prices  $B_n$  and  $Q_n$ , for all  $n \notin E$ , are such that optimal solutions for local problems satisfy, for all regions  $i$  and nodes  $n \notin E$ , the following:*

*L1. Unanimity. All regions agree on preferred global emissions  $e_n$*

$$e_n^i = e_n \quad \forall i \quad (8)$$

*L2. Balanced emissions. Optimal emissions of regions sum up to global emissions  $e_n$ :*

$$\sum_i e_{in} = e_n \quad (9)$$

*L3. Balanced net payments. The side-payments (net contributions) sum up to zero:*

$$\sum_i (P_n e_{in} - P_{in} e_n) = 0 \quad (10)$$

*L4. Balanced positions. Optimal positions of regions sum up to zero:*

$$\sum_i s_{in} = 0 \quad (11)$$



In this definition, accounting for (9), condition (10) is equivalently stated by

$$\sum_i P_{in} = P_n \quad (12)$$

which is consistent with the theory of public expenditure on collective consumption goods (Samuelson, 1954).

### 3.3 Existence, efficiency and computation of a Lindahl equilibrium

For the computation of a Lindahl equilibrium, we employ a convex and compact set of Negishi weights  $\Lambda = \{\lambda \geq 0 \mid \sum_i \lambda_i = 1\}$  in  $R^N$ . Given  $\lambda \in \Lambda$ , we consider the following *global problem* to find, for all  $i$  and  $n \notin E$ ,  $c_{in} \geq 0$ ,  $y_{in}$ ,  $e_{in}$  and  $z_{in}$ , and for all  $i$  and  $n$ ,  $k_{in}$  and  $x_n$ , to

$$\max \sum_i \lambda_i \sum_{n \notin E} \pi_n \rho_{in} v_i(c_{in}) \quad (13)$$

s.t.

$$\sum_i (c_{in} + z_{in} - y_{in}) = 0 \quad \forall n \notin E \quad (d_n) \quad (14)$$

$$k_{in} - \delta_k k_{in-} - z_{i,n-} = 0 \quad \forall n \quad (\nu_{in}) \quad (15)$$

$$-x_n + M(x_{n-}) + f \sum_i e_{i,n-} = g_{n-} \quad \forall n \quad (\mu_n) \quad (16)$$

$$y_{in} - \psi_{in}(k_{in}, l_{in}, e_{in}, x_{a,n}) \leq 0 \quad \forall n \notin E \quad (\eta_{in}) \quad (17)$$

Similar to local problems, the initial states  $k_{i0}$  and  $x_0$  are exogenous. The dual variables associated with the constraints are shown in parentheses.

Next, consider an optimal solution for the global problem (13)–(17) with optimal consumption  $c_{in}$ , output  $y_{in}$ , capital investment  $z_{in}$ , capital stock  $k_{in}$ , level of emissions  $e_{in}$  and environmental state  $x_n$ , for all regions  $i$  and nodes  $n$  as specified above. Let  $d_n$ ,  $\nu_{in}$ ,  $\mu_n$  and  $\eta_{in}$  denote optimal dual variables for (14), (15), (16) and (17), respectively. Then the following result shows that with a suitable choice of the Negishi weight vector  $\lambda$ , the global optimum yields local optimal solutions satisfying the conditions for a Lindahl equilibrium.

Given an optimal solution for the global problem, for each local problem (7) of region  $i$  and for all nodes  $n \notin E$ , define dual variables  $d_{in} = d_n$ , and  $\mu_{in}$  to satisfy dual feasibility

requirements (as seen by region  $i$ ) for the environmental state vector  $x_n$ . Thereafter, define for all  $i$  and  $n \notin E$

$$P_n = \sum_{n_+ \in S_n} \mu_{n_+} f / d_n \quad (18)$$

$$P_{in} = \sum_{n_+ \in S_n} \mu_{i,n_+} f / d_n \quad (19)$$

$$\Delta_{in} = c_{in} + z_{in} - y_{in} + P_n e_{in} - P_{in} e_n \quad (20)$$

$$r_i = \sum_{n \notin E} d_n \Delta_{in} \quad (21)$$

In (21), it can be shown that  $r_i/d_0$  is the net present value of the deficits  $\Delta_{in}$  evaluated by stochastic discounting factors<sup>19</sup>, and for short, we refer by *npv* to  $r_i$  defined in (21).

**Theorem 1.** *Assume A0, A1 and A2 hold and optimal solutions of the global and local problems exist with the definitions in (18)–(21). Then  $r_i = 0$ , for all  $i$ , implies*

(i) *for all regions  $i$ , globally optimal variables  $c_{in}$ ,  $z_{in}$ ,  $k_{in}$ ,  $x_n$ ,  $e_{in}$  and  $e_n = \sum_i e_{in}$ , with unanimously preferred global emissions  $e_n^i = e_n$ , are optimal for local problems (7), while financial positions  $s_{in}$  can be chosen to satisfy the budget balance (5).*

(ii) *such optimal local solutions constitute a Lindahl equilibrium with prices  $P_n$  in (18) and  $P_{in}$  in (19) such that  $\sum_i P_{in} = P_n > 0$ .*

Given a weight vector  $\lambda$ , let  $r = r(\lambda) \in R^N$  denote the npv vector. If  $r(\lambda) = 0$  then the vector  $\lambda$  *supports* a Lindahl equilibrium.

**Lemma 2.** *Given assumptions A0, A1 and A2, any Lindahl equilibrium is Pareto optimal with respect to expected utilities of regions.*

Lemma 2 asserts that regional utilities in a Lindahl equilibrium are such that no region can improve its utility without a sacrifice by other regions. Additionally, if  $C_n = \sum_i c_{in}$  is the global net output (consumption) in node  $n$ , then the following results shows that a Lindahl solution is also Pareto optimal with respect to total net outputs  $C_n$ ; i.e., the Lindahl solution is output efficient.

---

<sup>19</sup>See, e.g., Newell, Pizer and Prest (2022).

**Lemma 3.** *Given assumptions A0, A1 and A2, let  $C_n^* = \sum_i c_{in}^*$  be the global net output in node  $n$  in a Lindahl equilibrium. Then outputs  $C_n^*$  are optimal for maximizing  $\sum_n \iota_n C_n$  s.t. (14)–(17), for some weights  $\iota_n > 0$ .*

The first-best solution by a social planner (*SP*) is to maximize welfare over the regions over time, but as indicated by Lemma 3, there would be several potential interpretations of the weights that the optimization should use (for discussion, see, e.g., Hassler and Krusell, 2012). In Section 4 we opt for the maximization of the per capita utility of consumption over time so that the global problem (13)–(16) is retained but the objective (13) is replaced by

$$\max \sum_n \pi_n \rho_n \hat{L}_n \log(C_n/L_n) \quad (22)$$

where for all  $n$ ,  $C_n = \sum_i c_{in}$  is the total world consumption,  $L_n = \sum_i l_{in}$  is the total population, and parameters  $\hat{L}_n$  are positive. The following proposition shows an interdependence of the *SP* and Lindahl solutions.

**Lemma 4.** *For region  $i$  and node  $n$ , suppose the utility function of consumption  $c_{in}$  is  $v_i(c_{in}) = l_{in} \log(c_{in}/l_{in})$ , and the discounting factor  $\rho_{in} = \rho_n$  is independent of  $i$ . Assuming a Lindahl equilibrium with a supporting weight vector  $\lambda$  exists, let  $\hat{L}_n = \sum_i \lambda_i l_{in}$ . Then the *SP* solution with the objective (22) is identical with Lindahl's solution, except that regional consumption levels  $c_{in}$  may differ, although the total  $C_n = \sum_i c_{in}$  is the same for both.*

In Section 4 we use  $\hat{L}_n = L_n$  in (22) for the *SP* solution. Equivalently, this means using the arithmetic mean  $\hat{L}_n = L_n/N$  instead of the weighted average as in Lemma 4. Thereby, Lemma 4 yields the insight to understand why our *SP* solutions are very close to the Lindahl solutions.

Our iterative computation of an equilibrium is similar to Negishi (1972): in each iteration, (i) solve a global problem using Negishi weights  $\lambda \in \Lambda$  for regional objectives, (ii) evaluate Lindahl's prices and financial asset prices, (iii) construct solutions for the local problems and (iv) evaluate the npv, the net present values of the financial deficits, for all regions. If all net present values are zero, an equilibrium is found; otherwise, the Negishi weights are revised, and the next iteration begins.

The Algorithm for finding a Lindahl equilibrium proceeds over iterations  $\tau = 0, 1, 2, \dots$ . For updating the Negishi weights  $\lambda_i$  in iteration  $\tau$ , we use a relaxation parameter  $\theta_i > 0$  and a step-size parameter  $\kappa_\tau > 0$  where  $\theta_i$  is independent of  $\tau$  and  $\kappa_\tau$  is independent of  $i$ . In Appendix A we show how  $\theta_i$  can be determined. For the step size we assume

$$\lim_{\tau \rightarrow \infty} \kappa_\tau = \bar{\kappa} \quad \text{with } 0 < \bar{\kappa} < 1/2. \quad (23)$$

The steps of the Algorithm are as follows:

1. In iteration  $\tau = 0$ , take any  $\lambda^\tau \in \Lambda = \{\lambda \geq 0 \mid \sum_i \lambda_i = 1\}$ .
2. Solve the global problem (13)–(16) and compute  $\Delta_{in}$  in (20) using (18)–(19), for all  $i$  and  $n \notin E$ .
3. Compute the npv  $r_i^\tau = \sum_n d_n \Delta_{in}$  using (21), for all  $i$ .
4. If  $r_i^\tau = 0$ , for all  $i$ , then stop; a Lindahl equilibrium is found.
5. For each region  $i$ , with parameters  $\theta_i > 0$  and  $\kappa_\tau$  in (23), define

$$\hat{\lambda}_i = \lambda_i^\tau - \kappa_\tau \min(r_i^\tau, 0) / \theta_i \quad (24)$$

6. Scale  $\hat{\lambda}$  to obtain the update in  $\Lambda$ :

$$\lambda^{\tau+1} = \hat{\lambda} / \sum_i \hat{\lambda}_i \quad (25)$$

Replace  $\tau$  by  $\tau + 1$  and return to step 2.

In Appendix B we discuss convergence properties of the Algorithm. In Step 3 of the Algorithm, note that  $\sum_i r_i = 0$  by (9), (12) and (14). Hence, unless  $r_i = 0$ , for all  $i$  (in which case a Lindahl equilibrium is found by Theorem 1), at least one npv  $r_i$  is strictly negative. In order to ensure positive Negishi weights for the subsequent iteration, we only employ regions  $i$  in (24) such that  $r_i < 0$ . Note that  $\lambda^\tau > 0$  implies  $\lambda^{\tau+1} > 0$ . On the other hand, if  $\lambda_i^\tau = 0$  for some region  $i$ , then in the global optimum,  $c_{in} = 0$  is optimal for all  $n$  while other regions exploit the resources of region  $i$ . This leads to a negative npv  $r_i < 0$ , which in turn implies  $\lambda_i^{\tau+1} > 0$ .

The Algorithm defines a mapping  $\Gamma : \Lambda \rightarrow \Lambda$  for updating the Negishi weights on the weight simplex  $\Lambda$ . Iteration  $\tau$ , begins with some  $\lambda^\tau \in \Lambda$ , producing an npv vector  $r(\lambda^\tau)$ , and an updated weight vector  $\lambda^{\tau+1} = \Gamma(\lambda^\tau)$  to begin the subsequent iteration. We use this mapping to prove the existence of an equilibrium given the following additional assumption:

**Assumption A3:** (i) The feasible set of solutions for the global problem (13)–(17) is nonempty, (ii) the production functions are uniformly bounded such that  $0 < \psi_{in} \leq \bar{\psi}$  for all  $i, n$  and feasible solutions, and (iii) the transition mapping  $M(x)$  for the environmental state vector  $x$  is affine.

**Lemma 5.** *Given assumptions A0–A3, a Lindahl equilibrium exists.*

### 3.4 Lindahl equilibrium and emissions trading

Let  $w_{in}$  be the amount of emission permits initially allocated free of charge to region  $i$  at node  $n \notin E$  and let  $\theta_n$  denote the price of emission permits in the international market. If the emissions of region  $i$  at node  $n$  is  $e_{in}$  then the cash flow associated with emissions is  $\theta_n(w_{in} - e_{in})$ , and the problem of region  $i$  under emissions trade is as follows: For some weights  $\lambda_i > 0$  such that  $\sum_i \lambda_i = 1$ , given prices  $\theta_n$ , global emissions  $e_n = \sum_i w_{in}$  and financial market data  $B_n$  and  $Q_n$ , find  $c_{in}, y_{in}, z_{in}, k_{in}, e_{in}$  and  $s_{in}$  to

$$\max \lambda_i \sum_{n \notin E} \pi_n \rho_{in} v_i(c_{in}) \quad (26)$$

s.t.

$$c_{in} + z_{in} - y_{in} + \theta_n(e_{in} - w_{in}) + B_n s_{in} - Q_n s_{in-} = 0 \quad \forall n \notin E \quad (d_{in}) \quad (27)$$

$$k_{in} - \delta_k k_{in-} - z_{in} = 0 \quad \forall n \notin E \quad (\nu_{in}) \quad (28)$$

$$y_{in} - \psi_{in}(k_{in}, l_{in}, e_{in}, x_{a,n}) \leq 0 \quad \forall n \notin E \quad (\eta_{in}) \quad (29)$$

$$s_{in} = 0 \quad \forall n \in F.$$

Here global emissions  $e_n$  determine the environmental state  $x_n$  by (2) to be used in production functions  $\psi_{in}$ . Again, the initial capital  $k_{i0}$  and the preceding financial position  $s_{i0-}$  are exogenous for all  $i$ , and the dual variables associated with constraints are shown in parentheses.

At an equilibrium of the international emissions market (9) and (11) are satisfied. The following result generalizes the static and deterministic case by Mäler and Uzawa (1994).

**Lemma 6.** *Consider a Lindahl equilibrium with emission charge prices  $P_n$ , compensation prices  $P_{in}$ , and global emissions  $e_n$ , for all  $n \notin E$ . Suppose that the amounts  $w_{in}$  of emission permits initially allocated to regions  $i$  satisfy*

$$P_{in}e_n = P_n w_{in}. \tag{30}$$

*Then Lindahl's equilibrium is an equilibrium of the international emissions market with prices  $\theta_n = P_n$  of emission permits.*

## 4 Results

Our quantifications include both deterministic and stochastic experiments. A Lindahl equilibrium is found for each case, as well as social planner's solution (*SP*) and Cournot-Nash equilibrium for comparison. We use data for the 12 regions of RICE-2020<sup>20</sup>. Key modifications to RICE assumptions are steeper economic damages at temperatures above 2.5°C, endogenous choice of conventional technologies, and a climate model where the impact of emissions is materialized sooner. In addition, we introduce the negative emission technology<sup>21</sup>. Time horizon is from the base year 2015 until the terminal year 2200 and it is split into equal intervals of five years. We use 3% annual discounting for all regions.

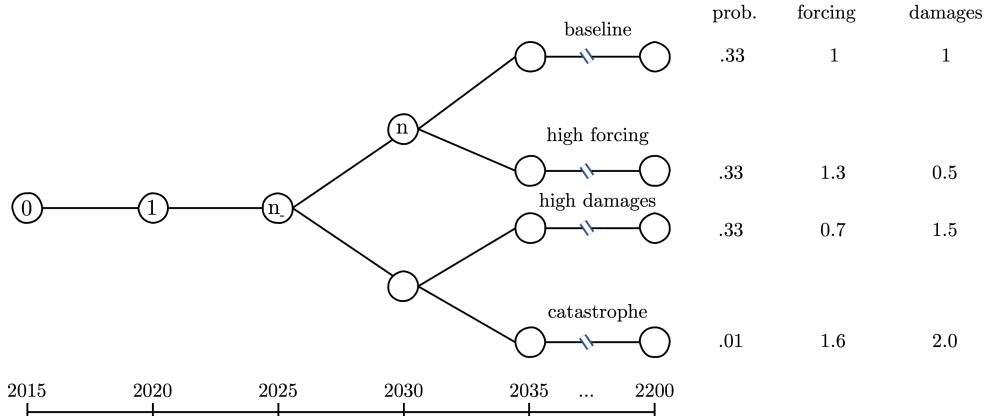
For the *SP* solution, we maximize the per capita utility of consumption over time: i.e., we maximize the objective in (22), weighted by  $\hat{L}_n = L_n$ , the total world population, subject to the global constraints. For the Cournot-Nash solution, we let the regions be autarkies where each region reacts other regions' emissions. Our computations are standard: starting with some initial emissions each region in turn takes the total emissions of other regions as given and finds its best response. We iterate until convergence.

---

<sup>20</sup>The 12 regions are: the U.S., Western Europe, Japan, other high income countries (*OHI*), Russia, Eastern Europe, China, India, the Middle East and North Africa (*MDE*), Sub-Saharan Africa, Latin America, and the rest of the world (*ROW*).

<sup>21</sup>Online Appendix B contains a detailed account of the changes.

**Figure 2:** Scenarios in the stochastic model.



Notes. The scenario tree has its the root node in year 2015 and time step is 5 years. The four scenarios start realizing in 2035; however, the first split is the tree is in 2030. *Baseline* shares the same parameters as the deterministic case. *High forcing* scenario has higher climate sensitivity with the forcing parameter  $\kappa$  in (88) increased by 30%, but economic damage function parameters  $a_{1,i}$  are 50% from their baseline values. In the *high damages* scenario, economic damages are more severe due to a 50% increase in the parameters  $a_{1,i}$ , but climate sensitivity is lowered with a 30% decrease in  $\kappa$ . Finally, a *catastrophe* scenario captures the possibility of a severe adverse outcome in both key uncertainties: the forcing parameter  $\kappa$  is increased by 60% and the damage parameters  $a_{1,i}$  are doubled. The probability for the *catastrophe* scenario is 1% while the other three scenarios are equally likely.

We begin with the baseline results assuming current technologies where negative emissions technologies are not available; thereafter, we consider the impact of possible Direct Air Capture technology (*DAC*). For computations, we use modeling software AMPL (Fourer, Gay and Keringham, 2003) with MINOS 5.5 -solver using default options (Murtagh and Saunders, 1978).

## 4.1 Baseline results

Table 1 summarizes our main results. Panel A gives our baseline quantifications which are restricted to abatement with current technologies only. The first three rows contrast the impact of the equilibrium concept; the comparison is between Cournot-Nash competition between the regions, the first-best (*SP*), and Lindahl’s equilibrium. All these scenarios are without uncertainty and have the same baseline parameters for climate sensitivity and economic damages. Table 1 also shows outcomes in Lindahl’s and Cournot equilibria under uncertainty that is captured by four distinct scenarios involving scaling of the temperature

forcing and economic damages parameters. For all model runs and scenarios, the percentage increases in the atmospheric carbon stock and atmospheric temperatures are presented for 2050, 2100, and 2150. The table also shows the social cost of carbon (SCC) for 2015 and 2050, as well as per capita annual consumption (net output) in 2150 and output relative to the benchmark based on the *SP* result.

Table 1, Panel A presents several findings. First, both first-best and cooperative solution offer marked improvements over competition between regions. In Cournot–Nash, slower action in emissions reductions results in higher increase in carbon stock, and, consequently, in higher temperatures and losses of ca. 6% in global output in 2150. In contrast, Lindahl’s equilibrium outcomes are almost indistinguishable from the first-best solution in our quantifications; this is explained by Lemma 4 and the related discussion.

Second result is that uncertainty increases the initial value of action now, as measured by the social cost of carbon, confirming the earlier similar findings in literature (e.g. Lemoine, 2021), at least with current technologies. As the uncertainty embedded in the scenarios unravels by 2050, in Lindahl’s equilibrium regions react strongly by adjusting the preferred global emissions levels, and as a result also the social cost of carbon. Scenarios that draw stronger climate sensitivities see emissions reduced whereas scenarios with lower forcing parameters allow larger carbon budgets going forward.

Third, the outcomes in terms of output loss are modest in all scenarios but the catastrophic one. These findings are in line with the origins of the model, see e.g. Nordhaus (2017), where the damages from climate change remain limited in comparison to economic growth<sup>22</sup>. However, using our sharper calibrations, if the most adverse outcome is realized, the damages are significant: a loss of one half (one third) of global output in the non-cooperative (cooperative) case by 2150. While our approach is different, the qualitative findings are in line with the stochastic growth simulations in Cai and Lontzek (2019).

Figure 3 decomposes the value of cooperation further across the range of future outcomes, measured in Cournot solution in proportion to Lindahl’s solution. Carbon concentrations (left panel) are higher in Cournot in all scenarios, but even non-cooperative regions start to restrict emissions more if a bad draw from climate sensitivity distribution is realized. Non-

---

<sup>22</sup>An update to the parameters of the related DICE-model is discussed in Barrage and Nordhaus (2023).



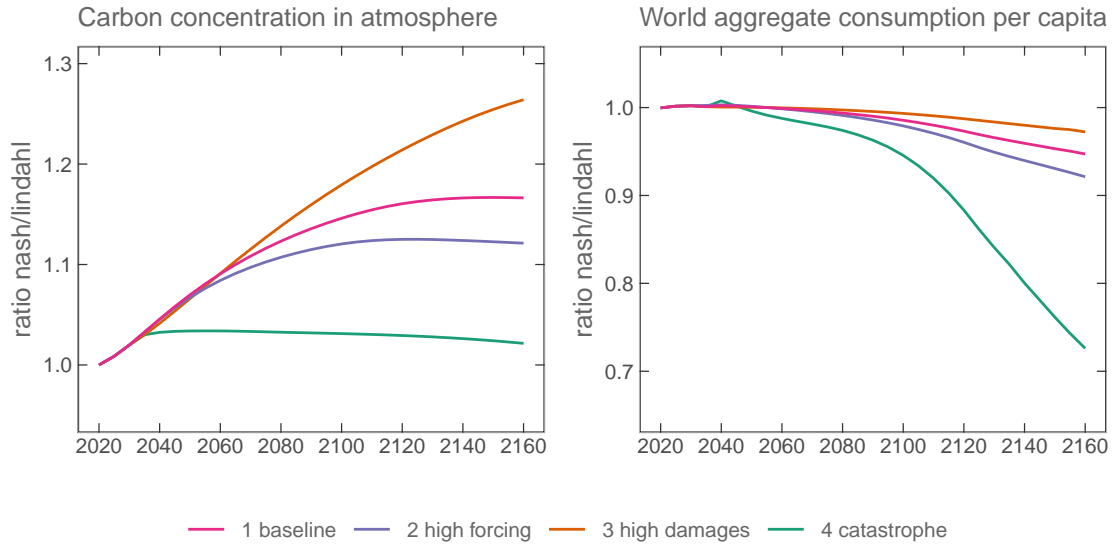
**Table 1:** Main results.

year	Temperature			$CO_2$ increase			SCC		Consumpt.	Output
	°C			%			\$/t $CO_2$		1000\$	%
	2050	2100	2150	2050	2100	2150	2015	2050	2150	2150
<i><b>Panel A.</b> Results with current technologies</i>										
Cournot (det.)	1.9	2.8	3.4	20	32	37	0	0	74	94.3
SP (det.)	1.6	2.3	2.8	11	13	16	92	337	79	100.0
Lindahl (det.)	1.7	2.3	2.8	11	14	17	93	341	79	100.3
Lindahl (stoch.)	1.7	2.3	2.8	11	14	17	101	387	79	99.9
1 baseline	1.6	2.3	2.8	11	13	16	101	333	79	100.7
2 high forcing	2.1	2.9	3.5	10	12	15	101	560	78	98.4
3 high damages	1.2	1.7	2.1	12	18	21	101	141	80	101.7
4 catastrophe	2.5	3.4	4.1	8	8	11	101	>1000	50	63.7
Cournot (stoch.)	1.8	2.8	3.4	19	31	39			75	94.5
1 baseline	1.8	2.8	3.3	18	30	36			75	95.1
2 high forcing	2.3	3.4	4.1	18	25	29			72	90.8
3 high damages	1.3	2.1	2.6	20	39	52			78	99.2
4 catastrophe	2.6	3.6	4.3	11	12	14			36	46.1
<i><b>Panel B.</b> Results when DAC technologies are available</i>										
Cournot (det.)	1.9	2.9	2.7	21	33	8	0	0	78	99.5
SP (det.)	1.7	1.8	0.9	13	-8	-32	66	193	82	103.5
Lindahl (det.)	1.7	1.8	0.9	14	-8	-32	66	193	82	103.7
Lindahl (stoch.)	1.7	1.8	1.0	14	-5	-31	64	182	81	103.2
1 baseline	1.7	1.8	0.9	14	-8	-32	64	193	81	103.2
2 high forcing	2.2	2.1	1.2	13	-13	-31	64	228	82	103.5
3 high damages	1.2	1.7	1.0	15	10	-26	64	118	81	103.2
4 catastrophe	2.3	0.8	0.1	-1	-35	-46	64	438	72	91.0
Cournot (stoch.)	1.9	2.8	2.8	21	33	17			79	99.6
1 baseline	1.9	2.9	2.7	21	33	8			78	99.4
2 high forcing	2.4	3.5	2.9	20	23	-4			79	100.7
3 high damages	1.4	2.2	2.7	23	44	50			78	98.7
4 catastrophe	2.8	2.6	1.6	16	-10	-30			80	101.7

Notes. The first three rows are from deterministic model runs with Cournot–Nash,  $SP$  (the first-best) and Lindahl’s allocation. For Lindahl and Cournot, the results from stochastic model run with four scenarios are included, the summary row for each presents the expected values. Outcome variables are annual values of selected years. For 2050, 2100 and 2150, the results show global mean temperature over the pre-industrialized era in degree Celsius, and the percentage increase of atmospheric  $CO_2$  stock relative to the base year 2015. For the years 2015 and 2050, the social cost of carbon (SCC) is measured in U.S. dollars per metric ton of carbon dioxide. Output is the annual consumption value in U.S. dollars per capita in 2150, and the relative value of output is compared to the deterministic  $SP$  (first-best) solution in percentage points.

cooperative regions consume slightly more initially (right panel), but this slower abatement leads to severe losses in total consumption later on, especially in the catastrophic outcome.

**Figure 3:** Cournot-Nash vs. Lindahl



Notes. The ratio figures from Cournot relative to Lindahl solutions for atmospheric carbon concentration (left panel) and the aggregated consumption (right panel) over time. The ratios are calculated by the scenario.

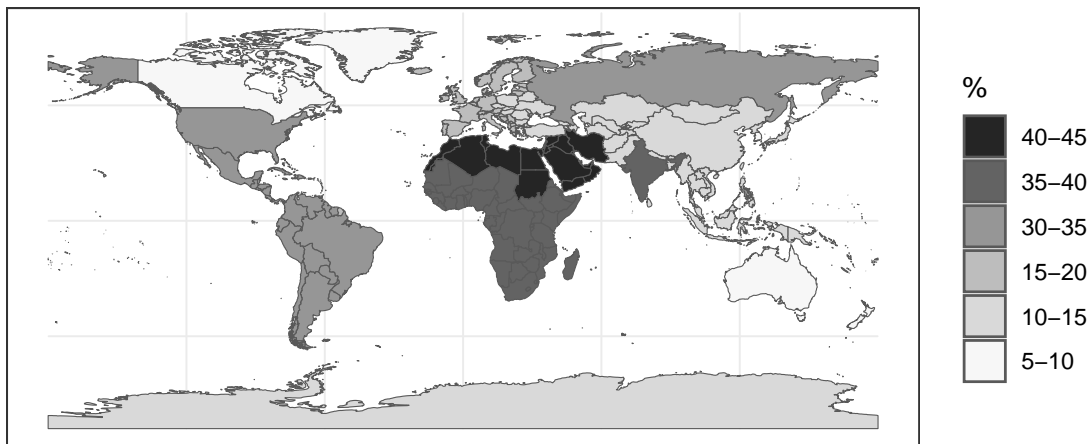
## 4.2 Regional breakdown of cooperation

Figure 4 offers a view of how relative gains from cooperation are distributed across the globe. The measure is constructed by first calculating the compensating variation that each region would be willing to pay to move from Cournot-Nash equilibrium to Lindahl’s allocation<sup>23</sup>. The absolute dollar value is largest in the U.S. (\$6 trillion), and the smallest in Eastern Europe (\$.4 trillion). For high-income regions combined, the value is estimated to be \$10 trillion while for other regions the total value is \$15 trillion. To make the valuations more comparable, we take two steps: First, we calculate the per capita dollar values using population estimates from 2015. Even when measured per capita, high income regions have around four times greater valuations than low and middle income regions. Second, we compare the per

<sup>23</sup>The precise values are calculated from bid price valuation as follows: Let  $u_i^*$  denote the expected present value of the utility function of region  $i$  in the Cournot–Nash equilibrium. We find the maximal price  $V_i$  which the region  $i$  is willing to pay such that the optimal utility after the payment  $V_i$  is at least  $u_i^*$ . For such optimization, we use the regional problems where the price  $V_i/\Delta$  is charged in the annual budget balance equation at the root node, the global emissions as well as the emissions prices  $P_n$  and  $P_{in}$ , and financial asset prices  $B_n$  and  $Q_n$  are given by the Lindahl equilibrium. More accurately, starting with financial market prices  $B_n$  and  $Q_n$  from the Lindahl equilibrium, we iterate to find adjusted prices which balance supply and demand in the financial market.

capita value to the purchase parity index adjusted annual gross national incomes (GNI)<sup>24</sup>. Such measure gives the highest relative valuation to the Middle East (that includes Northern Africa) and the least relative valuation to *OHI* (other high income countries). Regions with low per capita GNI (India and Sub-Saharan Africa) fare well in the comparison.

**Figure 4:** Beneficiaries of cooperation



Notes. The map represents the relative value of cooperation by the region. The gain from cooperation is the maximum price each region would pay to move from Cournot to Lindahl allocation in the deterministic model. These dollar amounts are converted to per capita values using 2015 population estimates. The percentages represent the ratio between the values and per capita annual gross national income of 2015 converted to international dollars using purchasing power parity rates.

There are two key mechanisms at play. The first channel is direct; the poorer regions suffer largest economic damages from the elevated temperatures of the non-cooperative world. The absolute present values are highest in China (\$34 trillion), India (\$23 trillion), the Middle East (\$26 trillion) and Latin America (\$25 trillion). The Lindahl solution avoids about half of the damage costs. Although the relative gain is similar in other regions, the absolute damages are smaller to begin with in the high income regions, e.g., the U.S. (\$12 trillion) or the EU (\$17 trillion), even though their economies are much larger.

The second channel of adjustment across regions comes from Lindahl's equilibrium compensations. In the cooperative outcome, it is mostly the poorer regions who receive personalized compensations based on global emissions, with China (\$6 trillion), India (\$4 trillion),

<sup>24</sup>Regional GNI is calculated as a population weighted average of the countries in the region. Data from World Bank Statistics.

Middle East (\$4 trillion), Latin America (\$4 trillion) and the region Rest of the World (*ROW*, \$5 trillion) ending up with the highest net compensations. As global tax revenues need to balance and efficiency gains alone cannot support payments, some regions are still net payers. These include the U.S. and most of the high income regions<sup>25</sup>.

The absolute values presented above are based on the deterministic model and 3% interest rate. The absolute magnitudes will be specific to the exact model specification, but valuations are bound to be significantly higher in catastrophic outcomes. Also, given that major savings from cooperation will occur after 2050, a decrease in the discounting rate would increase the gains substantially. In all model runs, the economic activity in emissions trading, investments, and financial markets seems rational, e.g., it is the high income regions that initially lend to the other regions.

### 4.3 Value of negative emissions technology

Even if all emissions/output ratios are set to zero, global temperatures continue to increase above the 1.5 °C level well before the end of the century and keep on increasing. The reason is that the initial carbon concentration of 850 Gt only reduces by about 2% by 2100. This observation motivates developing a large-scale negative emissions technology, such as Direct Air Capture (DAC), as a backstop technology. Indeed, National Academies of Sciences (2019) concludes: *"If the goals for climate and economic growth are to be achieved, negative emissions technologies will likely need to play a large role in mitigating climate change by removing ~10 Gt/y CO<sub>2</sub> globally by mid-century and ~20 Gt/y CO<sub>2</sub> globally by the century's end."*

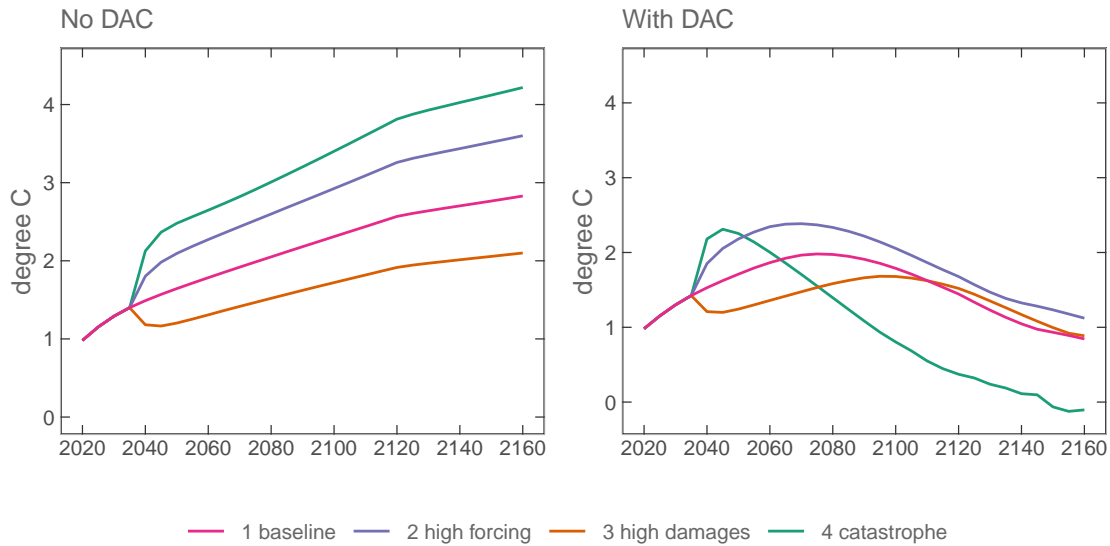
Table 1, Panel B shows summary results assuming DAC is available. Due to the high marginal costs of DAC, artificial carbon removals are deferred until the SCC increases high enough. Hence, the major impacts of DAC show up during the second half of the current century. Figure 5 displays the increase in atmospheric temperature for four scenarios in Lindahl's solution both with and without DAC. If DAC is not available, then the temperature

---

<sup>25</sup>Western Europe, China, and *ROW* are the interesting deviations here: Europe stands to gain net compensations on its emissions, this can be due to cleaner production technology. China and *ROW*, on the other hand, are going to be net payers despite the highest compensations.

increases by 2.1–4.1 °C by 2150. With DAC, Lindahl’s solution in 2150 is 1.2°C at the maximum; however, the temperature maxes at above 2°C because DAC deployment is not competitive during the first decades.

**Figure 5:** Impact of DAC to temperatures



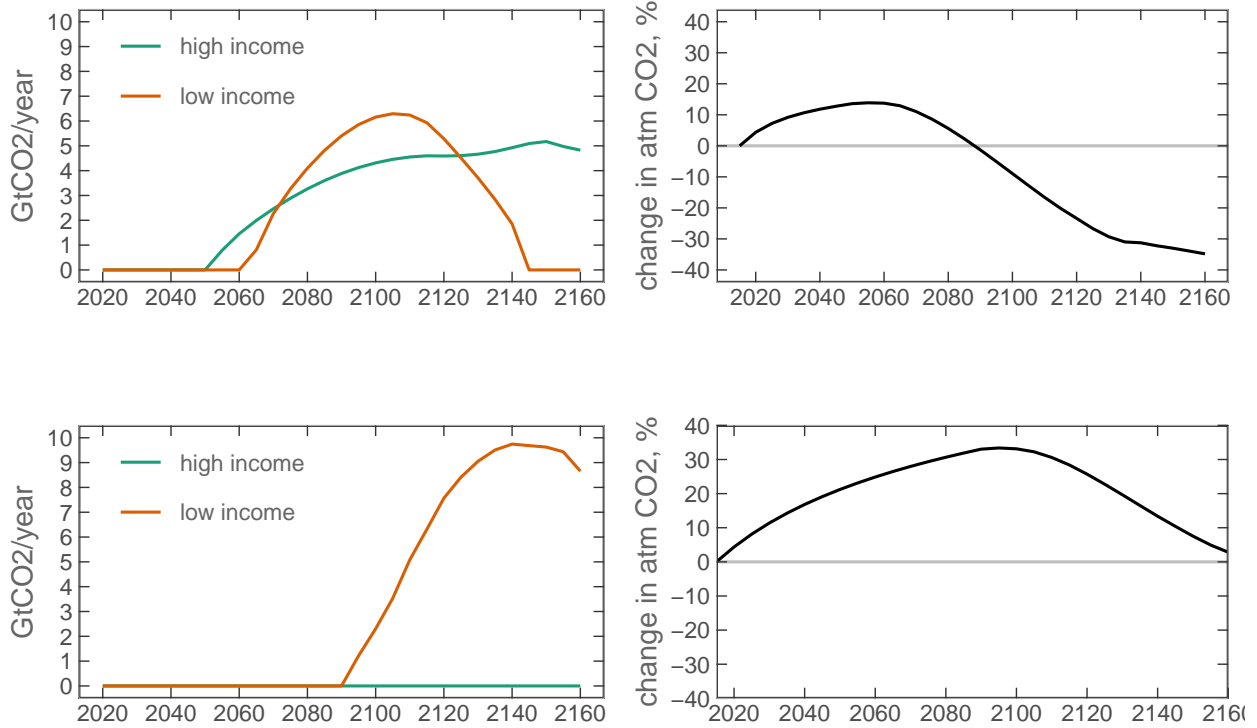
Notes. Temperature outcomes across scenarios in Lindahl’s equilibrium if no direct air capture (DAC) technology is available (left panel) or if the technology is available (right panel).

Figure 6 demonstrates the impact of cooperation on technology adoption in the baseline scenario of the stochastic model<sup>26</sup>. In Lindahl’s solution, the regions start to use DAC to reduce atmospheric carbon concentration around mid-century but the technology is taken up only by the end of the century when regions compete against each other. Interestingly, there is a marked difference in which regions start to employ DAC: In Cournot-Nash, it is only low and middle income regions that are forced to use the technology as their private marginal damages are higher. However, this removal of carbon from the atmosphere means that the higher income countries never need to respond. In Lindahl’s allocation, the technology is employed in a more balanced manner, with all regions contributing to abatement costs with DAC. This is the third channel where cooperation yields greater benefits to the poorer regions than the high income regions, if DAC technology is available.<sup>27</sup>

<sup>26</sup>The conclusions are quite similar for other scenarios, but the timing of DAC removals varies depending on the strength of forcing by scenario: decreased forcing postpones the start of DAC use.

<sup>27</sup>Intriguingly, in equilibrium, global carbon prices turn negative so that investments in DAC technology are indirectly funded by allowing increased emissions to the investing regions.

**Figure 6:** Use of DAC in the catastrophic scenario



Notes. Left: Amount of direct air capture (DAC) technology employed by the high income regions *HI* and the other (middle and low income) regions *MLI* in the deterministic model in Lindahl's equilibrium (top left panel) and Cournot equilibrium (bottom left panel); unit of measurement is metric gigatons of  $\text{CO}_2$  removed annually from the atmosphere. Right: The panels show the consequences in terms of percentage increase in the atmospheric  $\text{CO}_2$  concentration relative to base year levels in 2015 (Lindahl: top right panel, Cournot: bottom right panel)

We use real option valuation of arbitrage pricing theory to assess new technology development. If the technology works for certain, then from the stochastic model its value at present reaches \$8 trillion obtained as a bid the price based on *SP* solutions as specified in Lemma 4; from the deterministic model the value is \$6 trillion. However, these valuations drop almost linearly with the odds of DAC actually being successfully deployed. Obviously, much of the difference between the two valuations is extracted from avoiding the catastrophic scenario. The valuation is highly sensitive to the discounting rate used, if we change from our baseline 3% to 1.5%, the bid price value of the technology increases five-fold to \$39 trillion based on the stochastic model and to \$33 trillion in the deterministic model.

## 5 Concluding remarks

Unlike the quote at the top of the paper suggests, cooperative equilibrium concepts are not generally considered realistic as agreement is challenged by conflicts between stakeholders' private interests and trade-offs between future uncertainty and short-term costs. We may argue that climate negotiations are different as private information on global externalities has limits and physics will catch up with the free-riders in the end. Indeed, academic and policy discussions on climate court ideas of Lindahlian flavor<sup>28</sup>. Yet even if the global emissions scheme is out of reach in negotiations proper, our findings guide policy on three fronts.

First, purely self-centred decisions on emissions now force more costly abatement later on, and cooperation can benefit all regions across the range of uncertain futures we study. Second, in the case of catastrophic climate outcomes, a technology akin to the negative emission technology we study seems a necessity, and in expectation its present “insurance” value is measured in trillions of U.S. dollars. Third, in the long-run, all regions benefit from Lindhal’s allocation through the reduction of damages, and participation by everyone is attained through equilibrium compensations. Low- and middle-income regions also benefit from more evenly shared abatement costs. In a non-cooperative world, high income regions are more shielded from damages and can free-ride on low income regions’ abatement actions. One interpretation of our results is that the well-off countries could proxy the cooperative solution by offering to develop new radical technologies to contain damages, not unlike the proposals made for vaccine development in Kremer and Glennerster (2004), if in return all regions agree to moderate their short-term pollution. Politicians in wealthy nations may be more inclined to justify subsidies to technology development through induced domestic economic activity and spillover gains than by asking for billions in direct cash transfers.

Finally, we see also potential in revitalizing the study of Lindahl’s concept for other tangled global problems, biodiversity in particular (Dasgupta, 2021). In comparison to the climate problem, our understanding of how to deal with other global public goods is still in its infancy, offering a rich environment for research.

---

<sup>28</sup>E.g., by IMF in (Parry, Black and Roaf, 2021) where an idea of differentiated carbon floor prices for rich vs. poor countries is entertained.

## References

- Anthoff, David, and Johannes Emmerling.** 2019. “Inequality and the social cost of carbon.” *Journal of the Association of Environmental and Resource Economists*, 6(2): 243–273.
- Arrhenius, Svante.** 1896. “On the influence of carbonic acid in the air upon the temperature of the ground.” *The London, Edinburgh, and Dublin Philosophical Magazine and Journal of Science*, 41(251): 237–276.
- Baliga, Sandeep, and Eric Maskin.** 2003. “Mechanism design for the environment.” In *Handbook of environmental economics*. Vol. 1, 305–324. Elsevier.
- Barnett, Michael, William Brock, and Lars Peter Hansen.** 2022. “Climate change uncertainty spillover in the macroeconomy.” *NBER Macroeconomics Annual*, 36(1): 253–320.
- Barrage, Lint.** 2020. “Optimal dynamic carbon taxes in a climate–economy model with distortionary fiscal policy.” *The Review of Economic Studies*, 87(1): 1–39.
- Barrage, Lint, and William D Nordhaus.** 2023. “Policies, Projections, and the Social Cost of Carbon: Results from the DICE-2023 Model.” National Bureau of Economic Research.
- Barrett, Scott.** 2008. “The incredible economics of geoengineering.” *Environmental and resource economics*, 39: 45–54.
- Battaglini, Marco, and Bård Harstad.** 2020. “The political economy of weak treaties.” *Journal of Political Economy*, 128(2): 544–590.
- Berge, C.** 1963. *Topological Spaces*. Oliver and Boyd.
- Cai, Yongyang, and Thomas S Lontzek.** 2019. “The social cost of carbon with economic and climate risks.” *Journal of Political Economy*, 127(6): 2684–2734.
- Chichilnisky, Graciela, and Geoffrey Heal.** 1994. “Who should abate carbon emissions?: An international viewpoint.” *Economics Letters*, 44(4): 443–449.
- Chichilnisky, Graciela, Geoffrey M Heal, and David Starrett.** 1993. “International emission permits: equity and efficiency.” Department of Economics, Columbia University. Department of Economics Discussion Papers, 686.
- Crost, Benjamin, and Christian P Traeger.** 2014. “Optimal CO2 mitigation under damage risk valuation.” *Nature Climate Change*, 4(7): 631–636.
- Cruz, José Luis, and Esteban Rossi-Hansberg.** 2023. “The Economic Geography of Global Warming.” *Review of Economic Studies*.
- Dasgupta, Partha.** 2021. *The Economics of Biodiversity: The Dasgupta Review*. London: HM Treasury.



- Dietz, Simon, Frederick van der Ploeg, Armon Rezai, and Frank Venmans.** 2021. “Are economists getting climate dynamics right and does it matter?” *Journal of the Association of Environmental and Resource Economists*, 8(5): 895–921.
- Foley, Duncan K.** 1970. “Lindahl’s Solution and the Core of an Economy with Public Goods.” *Econometrica: Journal of the Econometric Society*, 66–72.
- Fourer, Robert, David Gay, and BV Keringham.** 2003. *AMPL: A Modeling Language for Mathematical Programming. Second Ed.* Duxbury-Thomson.
- Geoffroy, Olivier, David Saint-Martin, Dirk JL Olivié, Aurore Voldoire, Gilles Bellon, and Sophie Tytéca.** 2013. “Transient climate response in a two-layer energy-balance model. Part I: Analytical solution and parameter calibration using CMIP5 AOGCM experiments.” *Journal of Climate*, 26(6): 1841–1857.
- Gerlagh, Reyer, and Matti Liski.** 2016. “Carbon prices for the next hundred years.” *The Economic Journal*, 128(609): 728–757.
- Gillingham, Kenneth, William Nordhaus, David Anthoff, Geoffrey Blanford, Valentina Bosetti, Peter Christensen, Haewon McJeon, and John Reilly.** 2018. “Modeling uncertainty in integrated assessment of climate change: A multimodel comparison.” *Journal of the Association of Environmental and Resource Economists*, 5(4): 791–826.
- Golosov, Mikhail, John Hassler, Per Krusell, and Aleh Tsyvinski.** 2014. “Optimal taxes on fossil fuel in general equilibrium.” *Econometrica*, 82(1): 41–88.
- Groot, Loek, and Julia Swart.** 2018. “Climate change control: the Lindahl solution.” *Mitigation and adaptation strategies for global change*, 23(5): 757–782.
- Hassler, John, and Per Krusell.** 2012. “Economics and climate change: integrated assessment in a multi-region world.” *Journal of the European Economic Association*, 10(5): 974–1000.
- Hoel, Michael, and Kerstin Schneider.** 1997. “Incentives to participate in an international environmental agreement.” *Environmental and Resource Economics*, 9: 153–170.
- Jaakkola, Niko, and Frederick Van der Ploeg.** 2019. “Non-cooperative and cooperative climate policies with anticipated breakthrough technology.” *Journal of Environmental Economics and Management*, 97: 42–66.
- Jensen, Svern, and Christian P Traeger.** 2021. “Pricing climate risk.” CESifo Working Paper.
- Kaneko, Mamoru.** 1977. “The ratio equilibrium and a voting game in a public goods economy.” *Journal of Economic Theory*, 16(2): 123–136.
- Kotchen, Matthew J.** 2018. “Which social cost of carbon? A theoretical perspective.” *Journal of the Association of Environmental and Resource Economists*, 5(3): 673–694.

- Kremer, Michael, and Rachel Glennerster.** 2004. *Strong medicine: creating incentives for pharmaceutical research on neglected diseases*. Princeton University Press.
- Krusell, Per, and Anthony A Jr Smith.** 2022. “Climate change around the world.” National Bureau of Economic Research.
- Lemoine, Derek.** 2021. “The climate risk premium: how uncertainty affects the social cost of carbon.” *Journal of the Association of Environmental and Resource Economists*, 8(1): 27–57.
- Lindahl, Erik.** 1919. *Die Gerechtigkeit der Besteuerung: Eine Analyse der Steuerprinzipien auf Grundlage der Grenznutzentheorie*. Hakan Ohlssons Buchdruckerei.
- Liski, Matti, and Pauli Murto.** 2006. “Backstop technology adoption.” Helsinki Center of Economic Research Discussion Paper.
- Mäler, Karl-Göran, and Hirofumi Uzawa.** 1994. “Tradable emission permits, Pareto optimality, and Lindahl equilibrium.” Beijer Discussion Paper Series. Beijer Institute of Ecological Economics.
- Mas-Colell, Andreu, and Joaquim Silvestre.** 1989. “Cost share equilibria: A Lindahlian approach.” *Journal of Economic Theory*, 47(2): 239–256.
- Montero, Juan-Pablo.** 2008. “A simple auction mechanism for the optimal allocation of the commons.” *American Economic Review*, 98(1): 496–518.
- Murtagh, B, and M Saunders.** 1978. “Large-scale linearly constrained optimization.” *Mathematical Programming*, 14(1): 41–72.
- Murty, Sushama.** 2010. “Externalities and fundamental nonconvexities: a reconciliation of approaches to general equilibrium externality modeling and implications for decentralization.” *Journal of economic theory*, 145(1): 331–353.
- National Academies of Sciences, E.** 2019. “Negative emissions technologies and reliable sequestration: A research agenda.” National Academies of Sciences, Engineering, and Medicine.
- Negishi, Takashi.** 1972. *General equilibrium theory and international trade*. North-Holland Pub. Co.
- Newell, Richard G, William A Pizer, and Brian C Prest.** 2022. “A discounting rule for the social cost of carbon.” *Journal of the Association of Environmental and Resource Economists*, 9(5): 1017–1046.
- Nordhaus, William D.** 1973. “The allocation of energy resources.” *Brookings papers on economic activity*, 1973(3): 529–576.
- Nordhaus, William D.** 2017. “Revisiting the social cost of carbon.” *Proceedings of the National Academy of Sciences*, 114(7): 1518–1523.

- Nordhaus, William D, and Zili Yang.** 1996. “A regional dynamic general-equilibrium model of alternative climate-change strategies.” *The American Economic Review*, 741–765.
- Nordhaus, William D, and Zili Yang.** 2021. “The new DICE2020/RICE2020 modeling platform.” Mimeo.
- Parry, Ian, Simon Black, and James Roaf.** 2021. “Proposal for an international carbon price floor among large emitters.” International Monetary Fund Washington, DC.
- Pindyck, Robert S.** 2013. “Climate change policy: what do the models tell us?” *Journal of Economic Literature*, 51(3): 860–72.
- Rogelj, Joeri, Piers M Forster, Elmar Kriegler, Christopher J Smith, and Roland Séférian.** 2019. “Estimating and tracking the remaining carbon budget for stringent climate targets.” *Nature*, 571(7765): 335–342.
- Samuelson, Paul A.** 1954. “The pure theory of public expenditure.” *The review of economics and statistics*, 387–389.
- Sandmo, Agnar.** 2003. “International aspects of public goods provision.” *Providing Global Public Goods, Oxford University Press, Oxford*, 112–30.
- Shiell, Leslie.** 2003. “Equity and efficiency in international markets for pollution permits.” *Journal of Environmental Economics and Management*, 46(1): 38–51.
- Stanton, Elizabeth A.** 2011. “Negishi welfare weights in integrated assessment models: the mathematics of global inequality.” *Climatic Change*, 107(3): 417–432.
- Sundaram, R K.** 1996. *A first course in optimization theory*. Cambridge University Press.
- Terazono, Y, and A Matani.** 2015. “Continuity of optimal solution functions and their conditions on objective functions.” *SIAM Journal on Optimization*, 25(4): 2050–2066.
- Van der Ploeg, Frederick, and Aart de Zeeuw.** 2016. “Non-cooperative and cooperative responses to climate catastrophes in the global economy: A north–south perspective.” *Environmental and Resource Economics*, 65(3): 519–540.
- Varian, Hal R.** 1994. “A solution to the problem of externalities when agents are well-informed.” *The American Economic Review*, 1278–1293.
- Weikard, Hans-Peter, Michael Finus, and Juan-Carlos Altamirano-Cabrera.** 2006. “The impact of surplus sharing on the stability of international climate agreements.” *Oxford Economic Papers*, 58(2): 209–232.
- Weitzman, Martin L.** 2009. “Additive damages, fat-tailed climate dynamics, and uncertain discounting.” *Economics*, 3(1).
- Wets, Roger J-B.** 1989. “Chapter viii stochastic programming.” *Handbooks in operations research and management science*, 1: 573–629.

# Appendix

## A Estimating relaxation parameters $\theta_i$ for the Algorithm

For the relaxation parameters  $\theta_i$  in Step 5, consider the case based on log-utility  $v_i(c_{in}) = \log(c_{in})$ . After solving the global problem (13)–(16), define  $\delta_{in} = \Delta_{in} - c_{in}$ . Using optimality conditions for  $c_{in}$ , substitute  $c_{in} = \lambda_i \pi_n \rho_{in} / d_n$  and rewrite (21) as

$$r_i = \sum_n (\lambda_i \pi_n \rho_{in} + d_n \delta_{in}). \quad (31)$$

Solving for  $\lambda_i$  such that  $r_i = 0$  in (31), while keeping other parameters unchanged, yields

$$\hat{\lambda}_i = - \sum_n d_n \delta_{in} / \sum_n \pi_n \rho_{in},$$

where  $\sum_n d_n \delta_{in} = r_i - \lambda_i \sum_n \pi_n \rho_{in}$ . Hence, we rewrite

$$\hat{\lambda}_i = \lambda_i - r_i / \theta_i$$

where relaxation parameter is

$$\theta_i = \sum_n \pi_n \rho_{in}. \quad (32)$$

## B Convergence of the Algorithm

For the convergence of the Algorithm, we employ an intuitive assumption with strong empirical support. Given  $\lambda$ , the npv vector is  $r(\lambda) = r^c(\lambda) + r'(\lambda)$  where  $r_i^c$  accounts for the consumption of region  $i$  and  $r'_i$  takes care of the rest. An update in the weight vector to  $\lambda + \Delta\lambda$  (for a small increment  $\Delta\lambda$ ) merely leads to redistribution of consumption among regions while changes in the total net output is rather insignificant. Therefore, the major increment in the npv vector is due to changing consumption; i.e.,  $\Delta r_i = r_i(\lambda + \Delta\lambda) - r_i(\lambda) = \Delta r_i^c + \Delta r'_i$  where  $\Delta r'_i$  is small in comparison with  $\Delta r_i^c$ . In particular, we assume

$$\Delta r'_i < |\Delta r_i^c| \quad \forall i. \quad (33)$$

If  $\Delta r_i^c \leq 0$ , it follows from (33) that  $\Delta r_i^c + \Delta r'_i < 0$ , and if  $\Delta r_i^c > 0$ , then  $\Delta r_i^c + \Delta r'_i < 2\Delta r_i^c$ .

**Lemma 7.** *Assume A0–A3 and (33) hold true. For all  $i$ , let  $v_i(c) = \log(c)$  and let  $\theta_i = \sum_n \pi_n \rho_{in}$  be given by (32). Then, iterations  $\tau$  of the Algorithm with step-sizes  $\kappa_\tau$  satisfying (23) converge to a Lindahl equilibrium.*

**Remark:** The proof of Lemma 7 reveals an important consequence of assumption (33): the set of regions  $i$  with non-negative npv  $r_i^\tau$  converges over iterations  $\tau$  to a non-empty subset  $I_+$  and in the tail  $r_i^\tau$  is strictly decreasing for  $i \in I_+$ . Then  $\sum_{i \in I_+} r_i^\tau$  must converge to zero, implying  $r_i^\tau$  converges to zero for all  $i$  because  $\sum_i r_i^\tau = 0$ ; therefore, the algorithm converges to a Lindahl equilibrium by Theorem 1. However, we note that empirically (33) may be violated occasionally for some regions  $i$ ; nevertheless, in all of our numerical tests, the important consequences mentioned, and thereby convergence to a Lindahl equilibrium, remain valid.

## C Karush-Kuhn-Tucker (KKT) conditions

KKT conditions for the local problem of region  $i$ . For the local problems (7), Karush-Kuhn-Tucker (KKT) optimality conditions involve the primal constraints (2) - (6), one for each dual variable  $d_{in}$ ,  $\nu_{in}$ ,  $\mu_{in}$  and  $\eta_{in}$ , and a dual conditions, for each primal variable  $c_{in}$ ,  $y_n$ ,  $z_{in}$ ,  $k_{in}$ ,  $e_{in}$ ,  $e_n$ ,  $x_n$  and  $s_{in}$ . Denoting  $\psi_{in}^e = \partial\psi_{in}/\partial e_{in}$ ,  $\psi_{in}^x = \partial\psi_{in}/\partial x_n$ ,  $\psi_{in}^k = \partial\psi_{in}/\partial k_{in}$  and  $M_n = \partial M(x_n)/\partial x_n$ , the dual conditions are:

$$\lambda_i \pi_n \rho_{in} v'_i(c_{in}) - d_{in} = 0 \quad \forall n \notin E \quad (c_{in}) \quad (34)$$

$$d_{in} - \eta_{in} = 0 \quad \forall n \notin E \quad (y_{in}) \quad (35)$$

$$\left( \sum_{n_+ \in S_n} \nu_{i,n_+} - d_{in} \right) z_{in} = 0, \quad \sum_{n_+ \in S_n} \nu_{i,n_+} - d_{in} \leq 0 \quad \forall n \notin E \quad (z_{in}) \quad (36)$$

$$\eta_{in} \psi_{in}^k - \nu_{in} + \delta_k \sum_{n_+ \in S_n} \nu_{i,n_+} = 0 \quad \forall n > 0 \quad (k_{in}) \quad (37)$$

$$\eta_{in} \psi_{in}^e - d_{in} P_n = 0 \quad \forall n \notin E \quad (e_{in}) \quad (38)$$

$$d_{in} P_{in} - \sum_{n_+ \in S_n} \mu_{i,n_+} f = 0 \quad \forall n \notin E \quad (e_n^i) \quad (39)$$

$$\eta_{in} \psi_{in}^x + \mu_{in} - \sum_{n_+ \in S_n} \mu_{i,n_+} M_n = 0 \quad \forall n \quad (x_n) \quad (40)$$

$$d_{in} B_n - \sum_{n_+ \in S_n} d_{in_+} Q_{n_+} = 0 \quad \forall n \notin E \quad (s_{in}) \quad (41)$$

KKT conditions for the global problem. For the global problem (13)–(17), the optimality conditions comprise of the primal constraints (14)–(17), one for each dual variable  $d_n$ ,  $\nu_{in}$ ,  $\mu_n$  and  $\eta_{in}$ , and dual conditions (including complementarity) for all primal variables. For the primal variables  $c_n$ ,  $y_n$ ,  $z_n$ ,  $k_n$ ,  $e_{in}$  and  $x_n$ , the dual conditions are:

$$\lambda_i \pi_n \rho_{in} v'_i(c_{in}) - d_n \leq 0, \quad (\lambda_i \pi_n \rho_{in} v'_i - d_n) c_{in} = 0 \quad \forall n \notin E \quad (c_{in}) \quad (42)$$

$$d_n - \eta_{in} = 0 \quad (y_{in}) \quad (43)$$

$$\left( \sum_{n_+ \in S_n} \nu_{i,n_+} - d_n \right) z_{in} = 0, \quad \sum_{n_+ \in S_n} \nu_{i,n_+} - d_n \leq 0 \quad \forall n \notin E \quad (z_{in}) \quad (44)$$

$$\eta_{in} \psi_{in}^k - \nu_{in} + \delta_k \sum_{n_+ \in S_n} \nu_{in_+} = 0 \quad \forall n > 0 \quad (k_{in}) \quad (45)$$

$$\eta_{in} \psi_{in}^e - \sum_{n_+ \in S_n} \mu_{n_+} f = 0 \quad \forall n \notin E \quad (e_{in}) \quad (46)$$

$$\sum_i \eta_{in} \psi_{in}^x + \mu_n - \sum_{n_+ \in S_n} \mu_{n_+} M_n = 0 \quad \forall n > 0 \quad (x_n) \quad (47)$$

## D Proofs

*Proof. of Lemma 1.* Optimality condition (34) implies that weights  $\lambda_i$ , with  $\sum_i \lambda_i = 1$ , can be chosen such that  $d_{i0} = \lambda_i \rho_{i0} v_i(c_{i0}) = d_0 > 0$ , for all  $i$ . Condition (41) can be rewritten as  $d_{in} B_n = d_{in}^+ Q_n^+$ , where  $d_{in}^+$  is the row vector of dual variables  $d_{in_+}$ , for  $n_+ \in S_n$  and  $Q_n^+$  is the matrix with rows  $Q_{n_+}$ , for  $n_+ \in S_n$ . Assumption A2 implies that  $Q_n^+$  has full row rank. Hence, the dual variables  $d_{in_+}$ , for  $n_+ \in S_n$ , are uniquely determined by  $d_{in}$  and vectors  $B_n$  and  $Q_{n_+}$ . Inductively, if for the root node  $d_{i0} = d_0$  is independent of region, then for all nodes  $n$ ,  $d_{in} = d_n$  is independent of  $i$ . Furthermore, (34) implies  $d_{in} > 0$ .  $\square$

*Proof. of Theorem 1.* For (i), first, note that (42) implies  $d_n = \lambda_i \pi_n \rho_{in} v'_i(c_{in})$ , and hence,  $d_n > 0$  because  $\lambda_i \pi_n \rho_{in} > 0$  and  $v'_i > 0$ . Second, we need to verify the KKT conditions (5) - (6) and (34)–(41), for the local problems (7). Conditions (4)–(3) and (34)–(41), follow directly from the global KKT conditions (14)–(17) and (42)–(47) together with the definitions  $d_{in} = d_n$ ,  $\mu_{in}$  satisfying (40) with (35),  $P_n$  in (18),  $P_{in}$  in (19),  $e_n^i \equiv e_n = \sum_i e_{in}$ , and  $B_n$  and  $Q_n$  defined to satisfy the arbitrage pricing condition (41) with  $d_{in} = d_n > 0$ . The remaining KKT conditions are the local budget constraints (5) and terminal investment conditions (6).

To satisfy the budget balance (5) for  $n \notin E$ , we find suitable investments positions  $s_{in}$ . Using deficit  $\Delta_{in}$  in (20), constraints (5) are rewritten as follows:

$$-B_n s_{in} + Q_n s_{in_-} = \Delta_{in} \quad \forall n \notin E. \quad (48)$$

For redundant assets, which can be substituted by portfolios of other assets, we fix the positions in  $s_{in}$  to zero. Thereafter, for the non-redundant assets, we determine uniquely the investment positions recursively as follows. Recalling that  $S_n$  is the set of immediate successor nodes of  $n$ , for all time stages  $0 \leq t < T - 1$ , it follows from (48) that, for all nodes  $n$  in stage  $t$ ,

$$Q_{n_+} s_{in} = \Delta_{i,n_+} + B_{n_+} s_{i,n_+} \quad \forall n_+ \in S_n. \quad (49)$$

For  $n$  in stage  $T - 2$ ,  $n_+ \in F$ ,  $s_{i,n_+} = 0$  by (6), and by the complete market assumption A2, the non-redundant components in  $s_{in}$  are uniquely determined by (49). Similarly, for  $t = T - 3, \dots, 0$  and nodes  $n$  in stage  $t$ , we assume the positions in successor nodes  $S_n$  are already determined and we obtain the non-redundant components in  $s_{in}$ . Thereby, the chosen investment positions  $s_{in}$  satisfy (48), (5) and (6), for all nodes  $n \neq 0$ . Multiplying both sides of equation (48) by  $d_n > 0$  and summing over  $n \notin E$ , yields

$$\sum_{n \notin E} d_n (-B_n s_{in} + Q_n s_{in_-}) = \sum_{n \notin E} d_n \Delta_{in} = r_i \quad (50)$$

where the right side is  $r_i$  by (21). Because  $r_i = 0$ , it follows that (48) is satisfied for the root  $n = 0$  as well.

For (ii), first note that  $P_n > 0$ , because  $\sum_{n_+ \in S_n} \mu_{n_+} f = d_n \psi_{in}^e > 0$  by (43) and (46),  $d_n > 0$  and  $\psi_{in}^e > 0$  by assumption A1. Second, we need to verify Lindahl's equilibrium conditions (8)–(11), given the local optimal solutions in (i), and the prices  $P_n$  in (18) and  $P_{in}$  in (19). We already defined  $e_n = e_n^i = \sum_i e_{in}$  implying (8) and (9). Summing over  $i$  in (40) and accounting for (47) yields (inductively backwards)

$$\sum_i \mu_{in} = \mu_n. \quad (51)$$

Hence, (18) and (19) with (51) yield (12), which together with (9) imply (10). To show the remaining conditions (11), for all  $n \notin E$ , we use induction as follows. Summing over  $i$  on

both sides of (49) yields

$$Q_{n_+} \sum_i s_{in} = B_{n_+} \sum_i s_{i,n_+} \quad \forall n_+ \in S_n \quad (52)$$

because  $\sum_i \Delta_{i,n_+} = 0$  by (14) and (10). For all  $n$  at time stage  $T-2$  and  $n_+ \in S_n$ ,  $s_{i,n_+} = 0$  by (6). Hence,  $Q_{n_+} \sum_i s_{in} = 0$ , and consequently (because redundant components in  $s_{in}$  are fixed to zero),  $\sum_i s_{in} = 0$  by A2. Similarly, for the inductive steps, for  $n$  in stages  $T-3, \dots, 0$ , we assume  $\sum_i s_{i,n_+} = 0$ , for all  $n_+ \in S_n$ , to conclude  $\sum_i s_{in} = 0$ .  $\square$

*Proof. of Lemma 2.* It suffices to show that the primal variables  $c_{in}$ ,  $z_{in}$ ,  $k_{in}$ ,  $e_{in}$  and  $x_n$  from Lindahl equilibrium are optimal for the global problem (13)–(16) for some weights  $\lambda_i > 0$ . To see the primal feasibility, budget constraints (5) and equilibrium conditions (8)–(11) imply (14), (4) is identical to (15), (3) and (17) are identical, and (16) follows from (2) with (9). For the global dual requirements (42)–(47), based on Lemma 1, choose weights  $\lambda_i > 0$  such that, for all nodes  $n$ ,  $d_{in} = d_n$  is independent of region. Then (34)–(37) are identical to (42)–(45). If we define  $\mu_n = \sum_{in} \mu_{in}$ , then summing over  $i$  in (40) yields (47). Finally, (38), (39) and (12) imply (46).  $\square$

*Proof. of Lemma 3.* Let  $\lambda$  be the weight vector supporting the Lindahl equilibrium. Then the Lindahl solution is optimal for the global problem

$$\max \sum_{in} \lambda_i \pi_n \rho_{in} v_i(c_{in}) \quad \text{s.t. (14) – (17)}. \quad (53)$$

We show the assertion by three consecutive replacements of the objective function in (53) in such a way that the optimal solution remains unchanged. First, define  $a_{in} > 0$  such that  $a_{in}/c_{in}^* = \lambda_i \rho_{in} v_i'(c_{in}^*)$ , the scaled discounted marginal utility for  $i$  in  $n$ . Then the Lindahl solution is optimal for the following revised problem with log-utilities

$$\max \sum_{in} \pi_n a_{in} \log(c_{in}) \quad \text{s.t. (14) – (17)} \quad (54)$$

Denote by  $d_n$  the dual variable of the budget constraint (14). Then the optimality conditions for (54) imply  $a_{in}/c_{in} = a_{jn}/c_{jn} = d_n$  for all  $i, j$  and  $n$ . Consequently, denoting  $a_n = \sum_i a_{in}$ , we have  $a_{in}/c_{in} = a_n/C_n = d_n$ . Second, it follows that the Lindahl solution is optimal for



the following revised problem with log-utilities for  $C_n = \sum_i c_{in}$

$$\max \sum_n \pi_n a_n \log(C_n) \quad \text{s.t. (14) - (17)} \quad (55)$$

Third, to complete the proof, using linear approximation  $\log(C_n) \approx \log(C_n^*) + (C_n - C_n^*)/C_n^*$ , the Lindahl solution is optimal for the following revised problem

$$\max \sum_n \iota_n C_n \quad \text{s.t. (14) - (17)} \quad (56)$$

where  $\iota_n = \pi_n a_n / C_n^* > 0$  for all  $n$ . □

*Proof. of Lemma 4.* In the Lindahl equilibrium, let  $c_{in}^*$  denote the consumption of  $i$  in  $n$  obtained from an optimal solution of the global problem

$$\max \sum_{i,n} \pi_n \rho_n \lambda_i l_{in} \log(c_{in}/l_{in}) \quad \text{s.t. (14) - (17)} \quad (57)$$

Optimality conditions imply  $\pi_n \rho_n \lambda_i l_{in} / d_n = c_{in}$ , for all  $i$  and  $n$ . Summing over  $i$  yields

$$\pi_n \rho_n \hat{L}_n / d_n = \sum_i c_{in} = C_n \quad (58)$$

where  $C_n$  is the global consumption in node  $n$ . Maximizing  $\sum_n \pi_n \rho_n \hat{L}_n \log(C_n / L_n)$  in (22) subject to (14)–(17) leads to the optimality condition (58), and hence, the assertion follows. □

*Proof. of Lemma 5.* We show that a fixed point  $\lambda^* \in \Lambda$  exists for the mapping  $\Gamma : \Lambda \rightarrow \Lambda$  in (24)–(25). Then, by Theorem 1,  $\Gamma(\lambda^*) = \lambda^*$  implies a Lindahl equilibrium is found with Negishi weights  $\lambda^*$ . We show that  $\Gamma$  is continuous; then the assertion follows from Brouwer's fixed point theorem because  $\Lambda$  is convex and compact. Continuity of  $\Gamma$  is established in three steps as follows.

(i) For the global problem, we denote a solution by  $\xi = (c, y, z, k, e, x)$  where  $c = (c_{in})$ ,  $y = (y_{in})$ ,  $z = (z_{in})$ ,  $k = (k_{in})$ ,  $e = (e_{in})$  and  $x = (x_n)$ . The objective function in (13) is denoted by  $f(\xi, \lambda)$ . Assumptions A0–A3 imply that the global problem (13)–(17) is a convex optimization problem. Given that  $c \geq 0$ ,  $z \geq 0$ , and  $y$  is bounded above in (17) by assumption A3, it follows from (14) and A3 that the feasible set of solutions  $c$  is convex,

compact and non-empty. Therefore, an optimal solution for the global problem exists for all  $\lambda \in \Lambda$ . Furthermore, assumptions A0–A3 together with (14)–(17) and  $c, z \geq 0$  imply that the set of optimal solutions for the global problem is uniformly bounded over  $\lambda \in \Lambda$ . Therefore, there exists a convex and compact set (a box)  $B$  of solutions  $\xi$  such that  $B$  contains the optimal solutions for any given  $\lambda \in \Lambda$ . This in turn allows us to restrict the set  $\Xi^0$  of feasible solutions for (13)–(17) to a convex and compact set  $\Xi = \Xi^0 \cap B$ , independent of  $\lambda$ , such that  $\xi(\lambda)$  solves the restricted global problem  $\max_{\xi \in \Xi} f(\xi, \lambda)$  if and only if  $\xi(\lambda)$  is optimal for the global problem (13)–(17). Next, given  $\lambda \in \Lambda$ , we conclude that the global problem attains a unique optimal solution  $\xi(\lambda) \in \Xi$ .

- An optimal solution  $\xi = \xi(\lambda) \in \Xi$  for the global problem exists and the set of optimal solutions is convex.
- Based on assumption A0, for all  $i$  with  $\lambda_i = 0$ , the optimal consumption stream is  $c_i = (c_{in}) = 0$ , and for all  $i$  with  $\lambda_i > 0$ , the optimal consumption stream  $c_i$  is strictly positive and unique. Hence, the optimal consumption  $c$  is unique.
- Suppose the optimal output  $y = (y_{in})$  is not unique. Then there exist optimal solutions  $\xi^h$ , for  $h = 1, 2$ , and  $i, n$  such that  $y_{in}^1 = \psi_{in}(k_{in}^1, l_{in}, e_{in}^1, x_{a,n}^1) \neq y_{in}^2 = \psi_{in}(k_{in}^2, l_{in}, e_{in}^2, x_{a,n}^2)$ . A convex combination  $\xi^w$  of the two solutions, with weights  $w^h > 0$ , is optimal. However,  $y_{in}^w < \psi_{in}^w = \psi_{in}(k_{in}^w, l_{in}, e_{in}^w, x_{a,n}^w)$  by assumption A1. Hence, incrementing  $c_{in}$  and  $y_{in}^w$  by  $\psi_{in}^w - y_{in}^w > 0$  is feasible but leads to a contradiction because optimal  $c_{in}$  is unique. Therefore, optimal output  $y$  is unique.
- Similarly, by assumption A1, optimal scenarios of capital stock  $k = (k_{in})$ , emissions  $e = (e_{in})$ , and atmospheric temperatures  $x_{a,n}$ , for all  $n$ , are unique.
- Then, (15) implies  $z = (z_{in})$  is unique and (16) implies  $x = (x_n)$  is unique. Consequently, optimal  $\xi(\lambda)$  is unique.

(ii) Continuity of the optimal solution function  $\xi(\lambda)$  over  $\lambda \in \Lambda$  follows from Berge's maximum theorem<sup>29</sup> given the continuity of the objective function  $f(\xi, \lambda)$  on  $\Xi \times \Lambda$ , the

---

<sup>29</sup>See e.g., pp. 115–117 in Berge (1963), Corollary 9.20 on p. 239 in Sundaram (1996), and Theorem 3.1 in Terazono and Matani (2015).

convexity and compactness of the set  $\Xi$  which is nonempty and independent of  $\lambda$ , and the uniqueness of optimal solutions  $\xi(\lambda)$  shown in (i).

(iii) Accounting for (i) and (ii),

- condition (42) with A0 implies that optimal dual prices  $d_n$  are strictly positive and  $d_n$  is continuous on  $\Lambda$ .
- Then, condition (46) with A1 implies  $\sum_{n_+ \in S_n} \mu_{n_+} f = d_n \psi_{in}^e$  is continuous and  $P_n = \sum_{n_+ \in S_n} \mu_{n_+} f / d_n = \psi_{in}^e > 0$  is continuous on  $\Lambda$ .
- Given  $d_{in} = d_n$  and  $\eta_{in} = d_{in}$  by (35), (40) defines for all  $n$ ,  $\mu_{in} = -d_n \psi_{in}^x + \sum_{n_+ \in S_n} \mu_{in_+} M$ , where the matrix  $M$  defines the linear component of the affine the transition mapping in assumption A3. Thus, (40) defines (recursively) dual variables  $\mu_{in}$  which by A1 are continuous on  $\Lambda$  so that  $P_{in} = \sum_{n_+ \in S_n} \mu_{i,n_+} f / d_n$  is continuous, for all  $i$  and  $n$ .
- Thus,  $\Delta_{in}$  in (20) and  $r_i$  in (21) are continuous on  $\Lambda$ , for all  $i$  and  $n$ , and given constants  $\theta_i$  in (32),  $\hat{\lambda}_i$  in (24) is continuous on  $\Lambda$ .

Consequently,  $\Gamma(\lambda)$  in (25) is continuous on  $\Lambda$ . □

*Proof. of Lemma 6.* For the KKT optimality conditions, primal requirements are given by primal feasibility constraints (27)–(29), and the dual requirements with the associated primal variables in parentheses are as follows:

$$\lambda_i \pi_n \rho_{in} v'_i(c_{in}) - d_{in} = 0 \quad \forall n \notin E \quad (c_{in}) \quad (59)$$

$$d_{in} - \eta_{in} = 0 \quad \forall n \notin E \quad (y_{in}) \quad (60)$$

$$\nu_{in} - d_{in} = 0 \quad \forall n \notin E \quad (z_{in}) \quad (61)$$

$$\eta_{in} \psi_{in}^k - \nu_{in} + \delta_k \sum_{n_+ \in S_n} \nu_{in_+} = 0 \quad \forall n > 0 \quad (k_{in}) \quad (62)$$

$$\eta_{in} \psi_{in}^e - d_{in} \theta_n = 0 \quad \forall n \notin E \quad (e_{in}) \quad (63)$$

$$d_{in} B_n - \sum_{n_+ \in S_n} d_{in_+} Q_{n_+} = 0 \quad \forall n \notin E \quad (s_{in}) \quad (64)$$

Given the assumptions, equilibrium conditions for (2)–(29), (59)–(64), (9), (11) and  $s_{in} = 0$  for all  $n \in F$  in (6) follow directly from Lindahl equilibrium conditions.  $\square$

*Proof. of Lemma 7.* An equilibrium exists by Lemma 5. If convergence is finite, then the npv vector  $r^\tau = 0$ , for some iteration  $\tau$ , and the assertion follows from Theorem 1. Otherwise, for  $\tau = 0, 1, 2, \dots$ , consider iteration  $\tau$  starting with a weight vector  $\lambda^\tau$ , leading to an npv vector  $r^\tau$  and ending with a revised weight vector  $\lambda^{\tau+1}$ . For all  $\tau$ , let  $I_+^\tau = \{i | r_i^\tau \geq 0\}$ ,  $I_-^\tau = \{i | r_i^\tau < 0\}$  and  $I = I_+^\tau \cup I_-^\tau$ , the set of all regions. Let  $r_+^\tau = \sum_{i \in I_+^\tau} r_i^\tau$  and  $r_-^\tau = \sum_{i \in I_-^\tau} r_i^\tau$ , where  $r_+^\tau + r_-^\tau = 0$  because  $\sum_{i \in I} r_i^\tau = 0$ . Next, we show that  $r_+^{\tau+1} < r_+^\tau$  in the tail; i.e., the sequence  $\{r_+^\tau\}$  is strictly decreasing.

In iteration  $\tau$ , at an optimal solution of the global problem (13)–(16), (42) states

$$d_n = \lambda_i^\tau \pi_n \rho_{in} / c_{in} \quad \forall i \text{ and } n \notin E. \quad (65)$$

For region  $i$ , the consumption based component of the npv  $r_i^\tau$  in (20) and (21) is  $r_i^c = \sum_n d_n c_{in}$ . For the npv increment  $\Delta^{\tau+1} r_{in}$  in node  $n$  from iteration  $\tau$  to  $\tau + 1$ , condition (65) yields

$$\Delta^{\tau+1} r_{in}^c \equiv d_n^{\tau+1} c_{in}^{\tau+1} - d_n^\tau c_{in}^\tau = (\lambda_i^{\tau+1} - \lambda_i^\tau) \pi_n \rho_{in}.$$

Summing over  $n$  with (32) yields the npv increment

$$\Delta^{\tau+1} r_i^c = (\lambda_i^{\tau+1} - \lambda_i^\tau) \theta_i. \quad (66)$$

For  $i \in I_+^\tau$ , by (24) and (25) we have  $\lambda_i^{\tau+1} = \lambda_i^\tau / \omega_\tau < \lambda_i^\tau$ , where

$$\omega_\tau \equiv \sum_i \hat{\lambda}_i^\tau = 1 - \kappa_\tau \sum_{i \in I_-^\tau} r_i^\tau / \theta_i > 1. \quad (67)$$

Then, using (66) we have

$$\Delta^{\tau+1} r_i^c = (1/\omega_\tau - 1) \lambda_i^\tau \theta_i < 0$$

and using assumption (33),

$$r_i^{\tau+1} = r_i^\tau + \Delta^{\tau+1} r_i^c + \Delta^{\tau+1} r_i' < r_i^\tau \quad \forall i \in I_+^\tau \quad (68)$$

For  $i \in I_-^\tau$ , (24), (25), (66) and (67) yield

$$\Delta^{\tau+1} r_i^c = [(\lambda_i^\tau - \kappa_\tau r_i^\tau / \theta_i) / \omega_\tau - \lambda_i^\tau] \theta_i = -(\kappa_\tau / \omega_\tau) r_i^\tau + (1/\omega_\tau - 1) \lambda_i^\tau \theta_i$$

$$= -(\kappa_\tau/\omega_\tau)r_i^\tau + (\kappa_\tau/\omega_\tau)\lambda_i^\tau\theta_i \sum_{j \in I_-^\tau} r_j^\tau/\theta_j.$$

If  $\Delta^{\tau+1}r_i^c \leq 0$  and  $i \in I_-^\tau$ , then assumption (33) implies

$$r_i^{\tau+1} = r_i^\tau + \Delta^{\tau+1}r_i^c + \Delta^{\tau+1}r_i' < 0. \quad (69)$$

If  $\Delta^{\tau+1}r_i^c > 0$  and  $i \in I_-^\tau$ , then (23) implies that there is  $\tau'$  such that  $0 < \kappa_\tau < 1/2$  for all  $\tau > \tau'$ . Consequently, assumption (33) implies

$$\begin{aligned} r_i^{\tau+1} &= r_i^\tau + \Delta^{\tau+1}r_i^c + \Delta^{\tau+1}r_i' < r_i^\tau + 2\Delta^{\tau+1}r_i^c \\ &= r_i^\tau(1 - 2\kappa_\tau/\omega_\tau) + (2\kappa_\tau/\omega_\tau)\lambda_i^\tau\theta_i \sum_{j \in I_-^\tau} r_j^\tau/\theta_j < 0 \end{aligned} \quad (70)$$

where the inequality follows from the convex combination of two negative components.

For  $\tau > \tau'$  and for all  $i \in I_-^\tau$ , components  $r_i^{\tau+1}$ , are negative by (69)–(70) so that  $i \in I_-^\tau$  implies  $i \in I_-^{\tau+1}$ . Furthermore,  $r_i^{\tau+1} < r_i^\tau$  for all  $i \in I_+^\tau$  by (68); however, some components  $r_i^{\tau+1}$  may be negative and such  $i \in I_+^\tau$  is moved to  $I_-^{\tau+1}$ . Therefore, there is  $\bar{\tau} > \tau'$  such that, for all  $\tau > \bar{\tau}$ ,  $I_+^\tau = I_+$  and  $I_-^\tau = I_-$ , both sets independent of  $\tau$ . Consider iterations  $\tau > \bar{\tau}$ . Then for all  $i \in I_+$ , the sequence  $\{r_i^\tau\}_{\tau > \bar{\tau}}$  is non-negative and strictly decreasing by (68). Therefore  $r_i^\tau \rightarrow \bar{r}_i \geq 0$ , for all  $i \in I_+$ . Likewise,  $r_+^\tau = \sum_{i \in I_+} r_i^\tau \rightarrow \bar{r}_+ = \sum_{i \in I_+} \bar{r}_i$  and  $r_-^\tau = -r_+^\tau = \sum_{i \in I_-} r_i^\tau \rightarrow \bar{r}_- = -\bar{r}_+$ . Suppose that  $\bar{r}_+ > 0$ . Because  $-\sum_{i \in I_-} r_i^\tau = \sum_{i \in I_+} r_i^\tau > \bar{r}_+ > 0$ , there is  $\delta > 0$ , independent of  $\tau$ , such that for all  $\tau > \bar{\tau}$ ,  $-\sum_{i \in I_-} r_i^\tau/\theta_i > \delta$ . In iteration  $\tau > \bar{\tau}$ , for all  $i \in I_+$ , we have

$$\lambda_i^{\tau+1} = \lambda_i^\tau/\omega_\tau = \lambda_i^\tau/(1 - \kappa_\tau \sum_{i \in I_-} r_i^\tau/\theta_i) < \lambda_i^\tau/(1 + \kappa_\tau \delta)$$

Hence, for all  $i \in I_+$ ,  $\lambda_i^\tau$  converges to zero, because  $\prod_{\nu=\bar{\tau}}^\tau (1 + \kappa_\nu \delta) \rightarrow \infty$  by (23); a contradiction because  $\bar{r}_+ = -\bar{r}_- > 0$  cannot hold. Hence,  $\bar{r}_+ = \bar{r}_- = 0$  and the algorithm converges to a Lindahl equilibrium.  $\square$

# Online Appendix

## A model for global cooperation on climate change: Dynamic Lindahl equilibrium under uncertainty

Markku Kallio, Iivo Vehviläinen, and Hanna Virta

April 27, 2023

Corresponding author: Iivo Vehviläinen, [iivo.vehvilainen@aalto.fi](mailto:iivo.vehvilainen@aalto.fi)

### A Introducing Lindahl equilibrium via a static model

Two regions  $i = 1, 2$  consider cooperation on climate change. Both agree on the use of endogenous side-payments  $s_i$ ,  $i = 1, 2$ , paid by  $i$  to the other party; i.e.  $s_1 = -s_2$  where  $s_1$  may be positive or negative and  $\sum_i s_i = 0$ . Additionally, it is agreed that  $s_i = Pe_i - P_i e$ , where  $e_i$  is the emissions of  $i$ ,  $e = \sum_i e_i$  is total emissions,  $P$  is an emissions charge price (tax),  $P_i$  is a compensation price and  $\sum_i P_i = P$  because  $\sum_i s_i = 0$  and  $\sum_i e_i = e$ .

Let  $y_i$  be an exogenous output of  $i$  which creates exogenous gross emissions  $\sigma_i$ . The endogenous abatement is  $\sigma_i - e_i \geq 0$  with a cost  $\delta_i(\sigma_i - e_i)^2$  for region  $i$ . A damage cost  $\alpha_i e^2$  is due to total emissions creating a temperature increase<sup>30</sup>. The utility function of region  $i$  is  $u_i(c_i)$ , where  $c_i \geq 0$  is the consumption defined by output less abatement costs, damage costs and the side-payment; i.e.,

$$c_i = y_i - \delta_i(\sigma_i - e_i)^2 - \alpha_i e^2 - Pe_i + P_i e \quad (71)$$

The problem of region  $i$  is to find emissions  $e_i$  and the most preferred total emissions denoted by  $e^i$  to maximize  $u_i(c_i)$  s.t. (71) with  $e = e^i$ . Assuming  $u_i$  is increasing and strictly concave with  $u'_i \rightarrow \infty$  as  $c_i \rightarrow 0$ , the first order optimality conditions yield

$$e_i = \sigma_i - P/(2\delta_i) \quad (72)$$

$$e^i = P_i/(2\alpha_i). \quad (73)$$

---

<sup>30</sup>Arrhenius (1896) suggests an atmospheric temperature increase  $\kappa \log[(\bar{C} + e)/\bar{C}] \approx \kappa e/\bar{C}$ , where  $\kappa$  and  $\bar{C}$  are constants. Hence, the damage cost  $\alpha_i e^2$  is assumed proportional to the temperature increase squared.

In a Lindahl equilibrium, first, both regions prefer the same total emissions; i.e. for the optimal solutions,

$$e = e^i = P_i/(2\alpha_i) \quad i = 1,2 \quad (74)$$

which implies  $P_1/P_2 = \alpha_1/\alpha_2$ , and consequently  $P_i/P = \alpha_i/\sum_j \alpha_j$ . Thus, total emissions are

$$e = P/(2 \sum_j \alpha_j) \quad (75)$$

Second,  $e = \sum_i e_i$  implies

$$e = \sum_i [\sigma_i - P/(2\delta_i)] \quad (76)$$

which together with (75) yields the equilibrium charge price

$$P = 2 \sum_i \sigma_i / [\sum_i 1/\delta_i + 1/\sum_i \alpha_i]. \quad (77)$$

Thereafter, (74)–(75) yield the compensation prices

$$P_i = \alpha_i P / \sum_j \alpha_j. \quad (78)$$

For illustration, data is shown in Table A.2, including population  $l_i$ . Unanimity occurs with  $e = 0.9215$  Gt obtained from (75) with the charge price  $P = 55.29$  \$/t in (77).

**Table A.2:** Two-region example with parameters  $y_i$  (T\$),  $\sigma_i$  (Gt),  $\delta_i$  (M\$/(Mt)<sup>2</sup>),  $\alpha_i$  (M\$/(Mt)<sup>2</sup>) and  $l_i$  (millions).

$i$	$y_i$	$\sigma_i$	$\delta_i$	$\alpha_i$	$l_i$
1	16	1.4	0.024	0.01	320
2	20	2.8	0.013	0.02	1410

Lindahl (1919) introduces the equilibrium based on optimal responses of regions given the share of costs covered by each region. An equilibrium prevails if the parties are unanimous about the desired outcome of the environmental state - in our case, the atmospheric temperature determined by total emissions. In a similar spirit, Figure 1 illustrates the static model.

## B Implementing a stochastic and dynamic Lindahl model

Next, we introduce the implementation of the model for finding Lindahl equilibrium solutions for the numerical results of Section 4. The model underlying our stochastic programming formulation is the deterministic and dynamic 12-region model RICE-2020 (Nordhaus and Yang, 2021). In the implementation we introduce a more detailed representation of the economy compared to the Section 3. One potential concern may be the loss of convexity, true in theory, but we have not faced any computational issues in the implementation. The large number of regions seems sufficient to keep the non-convexities weak enough so that an unique equilibrium is consistently found<sup>31</sup>. The bulk of the data is adopted from RICE, including the choice of the base year 2015 and the time step  $\Delta = 5$  years<sup>32</sup>. We also introduce some modifications to the climatic and economic model in RICE, including uncertainty, the financial sector of Section 3, and others to be discussed below.

**Welfare function.** In RICE the welfare function (1) is based on log-utility:

$$u_i(c_i) = \sum_{t=0}^{T-1} \rho_t l_{it} \log(c_{it}/l_{it}) \quad (79)$$

where the discounting factor time stage  $t$  is  $\rho_t = (1 + R)^{-\Delta t}$  with  $R = 0.03$ , and  $l_{it}$  is an exogenously given population of region  $i$ . Thus the discounting is independent of regions and the single-period utility function  $v_i$  in (1) is  $v_i(c_{it}) = l_{it} \log(c_{it}/l_{it})$ .<sup>33</sup>

**Output.** In RICE, the annual output of region  $i$  in node  $n$  is  $y_{in} = y_{in}(k_{in}, l_{in}, h_{in}, x_n)$ , where the capital  $k_{in}$  is endogenous, the population  $l_{in}$  is a proxy for labor,  $x_n$  is the environmental state, and  $h_{in}$  is emissions abatement level to be defined shortly. Capital dynamics are as above in (4) with  $\delta_k = 0.9^\Delta$  where  $\Delta = 5$  years. The initial capital stock of the regions,  $k_{i0}$ , ranges from \$5 to \$50 trillion. Given an exogenous total factor productivity  $A_{in}$ , the output  $y_{in}^0$ , excluding damage and abatement costs, is given by a constant returns to scale

---

<sup>31</sup>A possible formal treatment of non-convexities could be pursued following standard techniques if the number of regions is large.

<sup>32</sup>Following RICE, unlike in Section 3, control variables in time stage  $t$  or node  $n$  refer to annual levels; for instance,  $e_n$  now is the total annual emissions during the five-year period starting at node  $n$ .

<sup>33</sup>In our implementation, the log-utility in (79) is used for relative risk aversion  $\alpha = 1$ , and for  $\alpha \neq 1$ , we have the power utility  $v(c_{it}) = \frac{l_{it}}{1-\alpha} (c_{it}/l_{it})^{1-\alpha}$  with  $\alpha > 0$ . In Section 4 we only report results for  $\alpha = 1$ .



production function

$$y_{in}^0 = A_{in} k_{in}^\gamma l_{in}^{(1-\gamma)} \quad (80)$$

with  $\gamma = 0.3$ , and the output  $y_{in}$  after damage and abatement costs is

$$y_{in} = y_{in}^0 \frac{1 - b_{1,i} h_{in}^{b_2}}{1 + a_{1,i} [T_{a,n}/T_0]^{a_2}}. \quad (81)$$

In (81), the denominator accounts for the damage costs relative to output related to an increase  $T_{a,n}$  in atmospheric temperature above pre-industrial level (the component  $x_{a,n}$  in the environmental state vector  $x_n$ ), and  $T_0 = 2.5$  ( $^{\circ}\text{C}$ ) is an exogenous reference level. Parameters  $a_{1,i}$ , ranging from 1% to 2%, reveal the share of output lost is case the temperature increase is at the reference level; i.e.,  $T_{a,n} = T_0$ .

The emissions/output ratio  $\sigma_{in}$  is exogenous and an endogenous emission control rate  $h_{in} \leq 1$  defines the abatement share of the emissions; thereafter, the remaining output related emissions are  $(1 - h_{in})\sigma_{in}y_{in}^0$ . The abatement cost in (81) relative to output is  $b_{1,i}h_{in}^{b_2}$ . Parameters  $b_{1,i}$ , ranging from 5% to 10%, define the share of output lost is in the extreme case of  $h_{in} = 1$  resulting in zero emissions from output.

We revise (81) in two ways. First, following Weitzman (2009), the damage loss function may be replaced by  $\exp(\beta_i T_{a,n}^2)$  which improves the sensitivity to large temperature increases. Parameters  $\beta_i$  are chosen such that the cost at  $T_{a,n} = T_0$  is the same as the damage cost in RICE. As an alternative, we consider a revised damage function  $(1 + a_{1,i} \exp[\beta(T_{a,n} - T_0)])$  with  $\beta = a_2$ . The two damage functions have the similar characteristics; however, the latter reacts more strongly to temperature increases above 3  $^{\circ}\text{C}$  and is also more suitable for numerical optimization. Figure B.7 (left) displays the RICE and the revised damage cost functions, for which the costs are equal for  $T_{a,n} = T_0$ . Second, for artificial carbon sinks we consider possible new carbon absorbing technologies, such as direct air capture (DAC)<sup>34</sup>, for removing carbon from the atmosphere to be stored in suitable sinks. The cost of carbon absorption relative to output is  $d_{1,i}q_{in} + d_{2,i}q_{in}^{d_3}$  where the first (linear) component prevents the exploitation of this technology in case of a low carbon tax and the second progressively increasing component limits the availability<sup>35</sup>. Figure B.7 (right) displays abatement and

<sup>34</sup>IEA estimates 1 Gt/yr capture by DAC in 2050.

<sup>35</sup>The DAC cost parameters are calibrated to envisioned carbon absorption cost for DAC: we use  $d_{1,i} = 0.08$

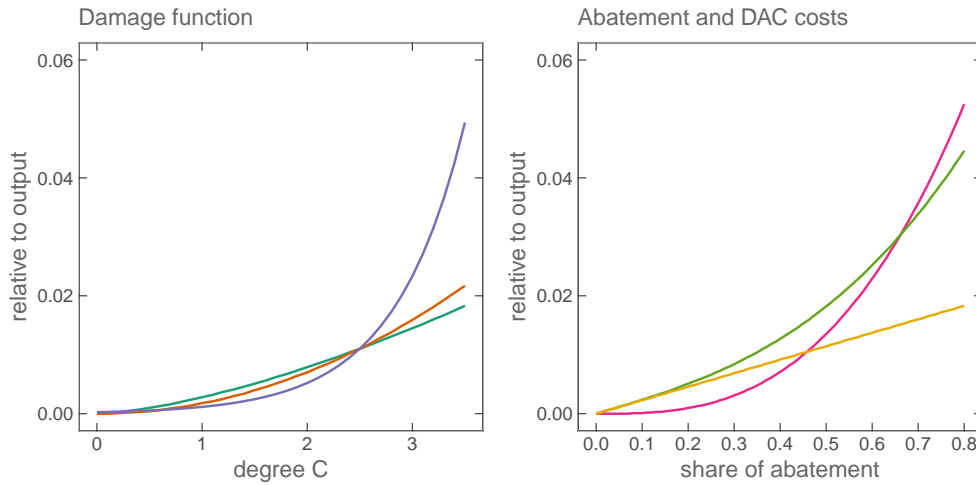
DAC cost functions. DAC becomes competitive when its marginal cost in \$ per ton of carbon falls below the one for abatement.<sup>36</sup>

Similarly as for abatement  $h_{in}$ , an endogenous parameter  $q_{in}$  defines the level of removal in proportion to emissions  $\sigma_{i0}y_{in}^0$  based on the initial emissions/output ration  $\sigma_{i0}$ ; i.e., the quantity of carbon captured to the sink is  $q_{in}\hat{\sigma}_i y_{in}^0$  where parameters  $\hat{\sigma}_i$  are constants. Thereby, (81) is replaced by

$$y_{in} = y_{in}^0 \frac{(1-b_{1,i}h_{in}^{b_2})(1-d_{1,i}q_{in}-d_{2,i}q_{in}^{d_3})}{1+a_{1,i} \exp[\beta(T_{a,n}-T_0)]}. \quad (82)$$

Finally, the annual output is then  $y_{in} = y_{in}(k_{in}, l_{in}, h_{in}, q_{in}, x_n)$ .

**Figure B.7:** Cost assumptions.



Notes. Left panel: Three damage cost functions; the function in RICE (green), the revised function (blue) and Weitzman's exponential function (orange). Right: Abatement and DAC cost functions; the abatement cost (red), the DAC cost (green) and the linear component the DAC (yellow). All costs are relative to output.

**Emissions.** In RICE, the annual emissions  $e_{in}$  of region  $i$  in node  $n$  are determined by exogenous emissions output ratios  $\sigma_{in}$ , annual output, the level  $h_{in}$  of abatement, and exogenous for high income regions  $i$ , and  $d_{1,i} = 0.10$  for all other regions; for the other cost parameters,  $d_{2,i} = 0.5 \cdot b_{1,i}$  and  $d_3 = b_2$ .

<sup>36</sup>Note that equal slopes in the two curves in Figure B.7 do not reveal the brak-even point directly because the fractions (levels) in horizontal axis refer to different quantities of CO<sub>2</sub>:  $\sigma_{in}y_{in}^0$  for abatement and  $\hat{\sigma}_i y_{in}^0$  for DAC.

annual emissions  $e_{in}^0$  of land and forests; global emissions  $e_n$  are the sum over regions:

$$e_{in} = (1 - h_{in})\sigma_{in}y_{in}^0 + e_{in}^0 \quad \forall i, n \quad (83)$$

$$e_n = \sum_i e_{in} \quad \forall n \quad (84)$$

The emissions/output ratios  $\sigma_{in}$  range from 0.05 to 0.15 in 2015 and from 0.02 to 0.06 in 2100 (all ratios are in Gt/T\$). When we account for the artificial carbon absorption  $q_{in}\hat{\sigma}_iy_{in}^0$ , we use  $\hat{\sigma}_i = 0.1$ , for all  $i$ , and (83) is replaced by

$$e_{in} = [(1 - h_{in})\sigma_{in} - q_{in}\hat{\sigma}_i]y_{in}^0 + e_{in}^0. \quad (85)$$

As mentioned, the ratios  $\sigma_{in}$  are exogenous in RICE. However, the choice of abatement level  $h_{in}$  needs an investment in production technology and we assume such technology stays available in subsequent periods as well. Therefore, we consider endogenous emissions/output ratios controlled by the abatement levels  $h_{in}$  as follows;

$$\sigma_{in} = (1 - h_{i,n-})\sigma_{i,n-}. \quad (86)$$

For simplicity, we exclude depreciation and assume the maintenance cost of the improved technology is included in the cost of adopting the abatement level  $h_{in}$ .

**Environmental dynamics.** In RICE, the equation (2) for the environmental state vector  $x_n$  defines the carbon cycle and temperature dynamics as follows. For carbon cycle, there are three stocks of carbon in  $x_n$  at each node  $n$ :  $C_n^A$  is the carbon concentration in the atmosphere (Gt),  $C_n^L$  is the carbon concentration in lower oceans (Gt), and  $C_n^U$  is the carbon concentration in shallow oceans (Gt). Denoting  $C_n = (C_n^A, C_n^L, C_n^U)$ , the carbon cycle model is

$$C_n = C_{n-}M + (\Delta \cdot e_{n-}, 0, 0) \quad (87)$$

where  $M$  is a given transition matrix and  $\Delta \cdot e_{n-}$  is the increment by emissions  $e_{n-}$  of CO<sub>2</sub> in the atmosphere in  $\Delta$  years. The initial stock levels in the base year 2015 are  $C_0^A = 851$  Gt,  $C_0^L = 1740$  Gt,  $C_0^U = 460$  Gt.

The other two endogenous components in the environmental state vector  $x_n$  are the atmospheric temperature  $T_{a,n}$  and the ocean temperature  $T_{o,n}$  (both in °C above the historical

level). The level of radiative forcing  $F_n$  (Arrhenius, 1896) is

$$F_n = \kappa \log(C_n^A/\bar{C}) + F_{o,n} \quad (88)$$

where  $\kappa = 5.92 \text{ W/m}^2$  in RICE,  $C_n^A$  is as above (the quantity of  $\text{CO}_2$  in the atmosphere),  $\bar{C} = 596 \text{ Gt}$  is the pre-industrial  $\text{CO}_2$  concentration, and  $F_{o,n}$  is an exogenous forcing component. The temperature dynamics is given by a linear system of equations:

$$T_{a,n} = H_0 F_{n_-} + H_1 T_{a,n_-} - H_a (T_{a,n_-} - T_{o,n_-}) \quad \forall n > 0 \quad (89)$$

$$T_{o,n} = T_{o,n_-} + H_o (T_{a,n_-} - T_{o,n_-}) \quad \forall n > 0 \quad (90)$$

where the exogenous parameters are  $H_0 = 0.050 \text{ (}^\circ\text{C m}^2/\text{W)}$ ,  $H_1 = 0.934$ ,  $H_a = 0.00126$  and  $H_o = 0.0125$ . The initial values in the base year 2015 are  $T_{a,0} = 0.85 \text{ }^\circ\text{C}$  and  $T_{o,0} = 0.0068 \text{ }^\circ\text{C}$ .

We reformulate (89)–(90) to account for the more recent scientific take on climate sensitivity. From Geoffroy et al. (2013), the temperature dynamics for atmospheric temperature  $T_a$  and ocean temperature  $T_o$  follow the differential equations

$$C_a \frac{dT_a}{dt} = F - \lambda T_a - \gamma (T_a - T_o) \quad (91)$$

$$C_o \frac{dT_o}{dt} = \gamma (T_a - T_o) \quad (92)$$

Integrating (91)–(92), and assuming the forcing  $F$  is constant from node  $n_-$  to  $n$ , (89)–(90) are replaced by

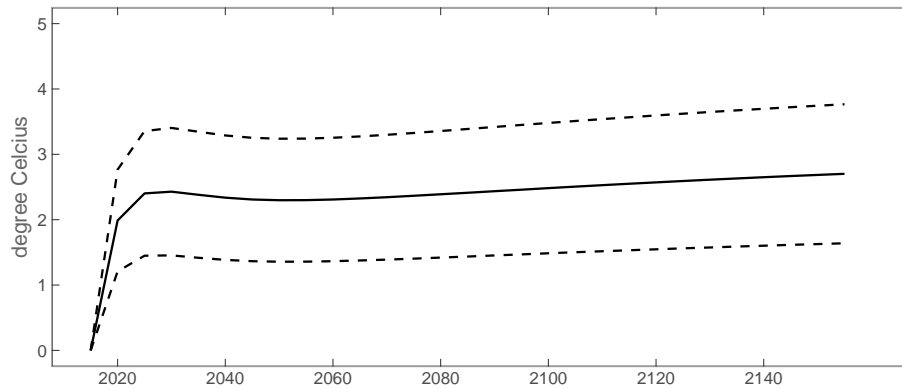
$$T_{a,n} = A_{a,0} F_{n_-} + A_{a,1} T_{a,n_-} + A_{a,2} T_{o,n_-} \quad \forall n > 0 \quad (93)$$

$$T_{o,n} = A_{o,0} F_{n_-} + A_{o,1} T_{a,n_-} + A_{o,2} T_{o,n_-} \quad \forall n > 0 \quad (94)$$

For parameters  $C_a$ ,  $C_o$ ,  $\lambda$  and  $\gamma$  we use averages over 16 studies as reported by Geoffroy et al. (2013). Parameters  $A_{a,0}, \dots, A_{o,2}$  in (93) and (94) are independent of time and state of node  $n$ . Figure B.8 show the increase in atmospheric temperature over a hundred years as a response to an increase of the initial  $\text{CO}_2$  stock  $C_0^A$  by 1 teraton and omitting all other subsequent emissions, including forest, land and industrial emissions. The short term increase in temperature is about  $2.4 \text{ }^\circ\text{C}$ , a results which is in line with those reported in other studies; see e.g., Hansen et al. (2022). Figure B.8 shows also the response assuming a

30% increase or decrease in the forcing parameter  $\kappa$  in (88); such variations are used in our scenarios of Section 4 to study the uncertainty on climate warming.

**Figure B.8:** Climate response.



Notes. Climate response ( $^{\circ}\text{C}$ ) due to 1 teraton increase in the initial  $\text{CO}_2$  concentration in the atmosphere. The middle line is the base case; in the two other cases, the forcing is changed by -30% and +30% relative to the base case.